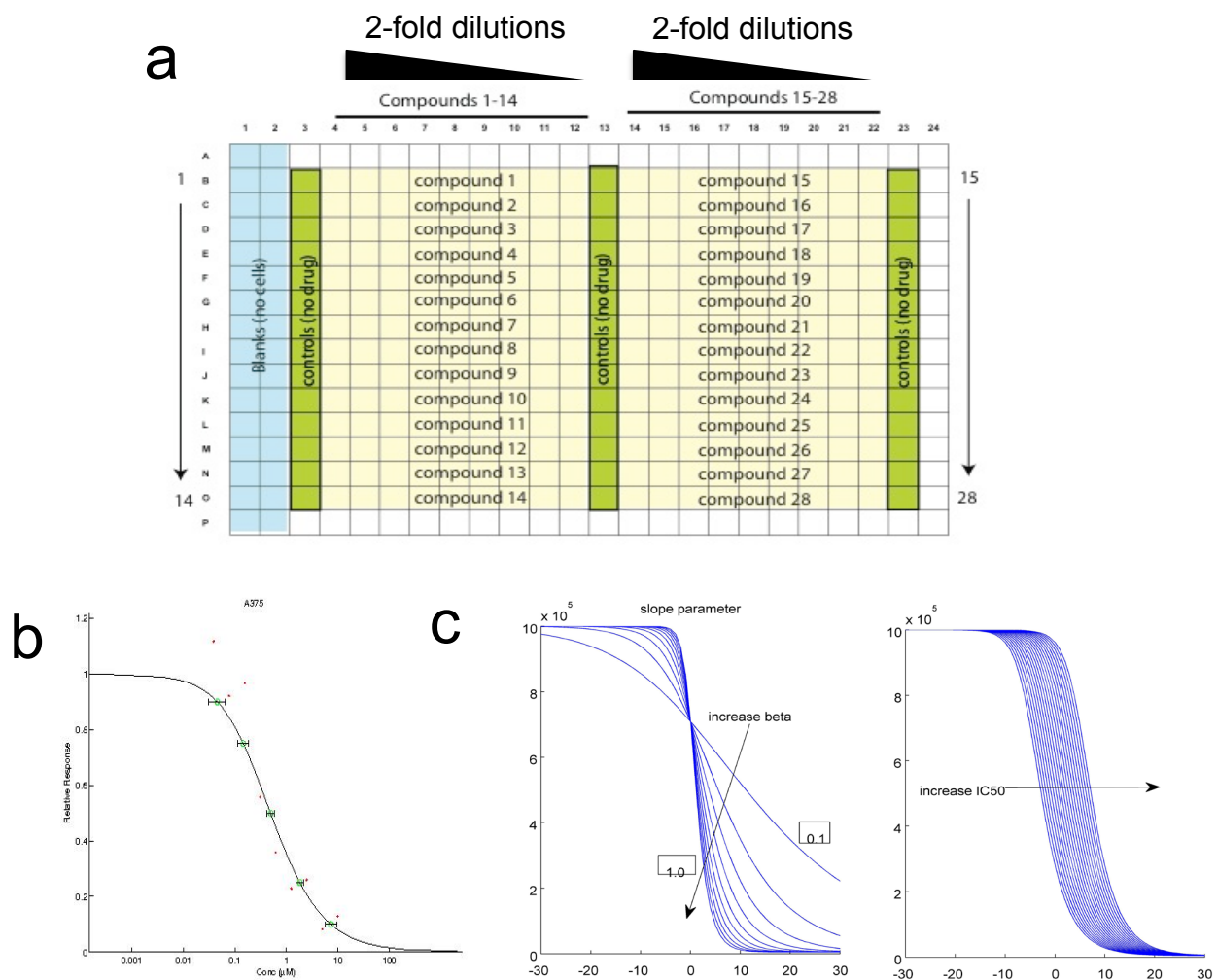
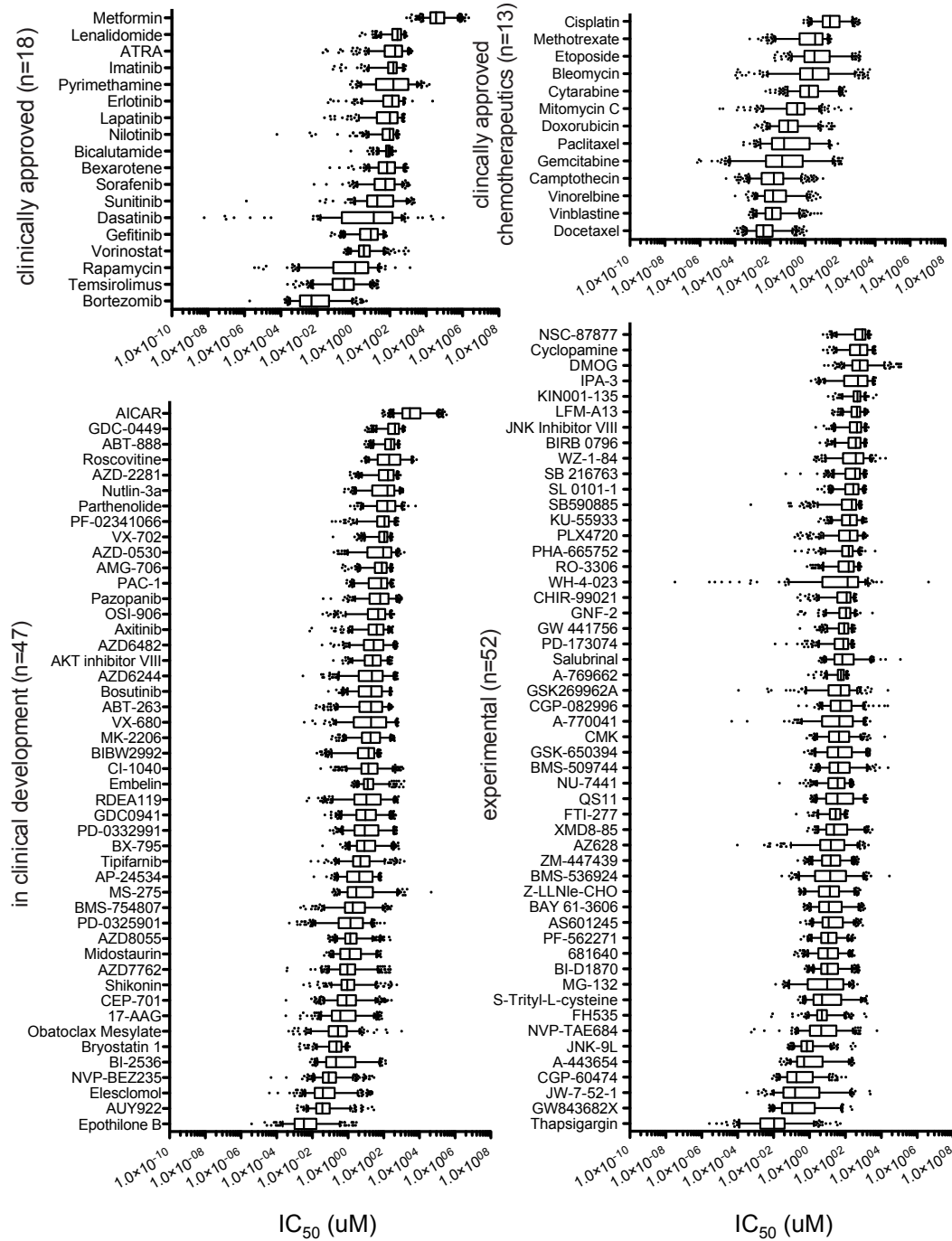


SUPPLEMENTARY INFORMATION

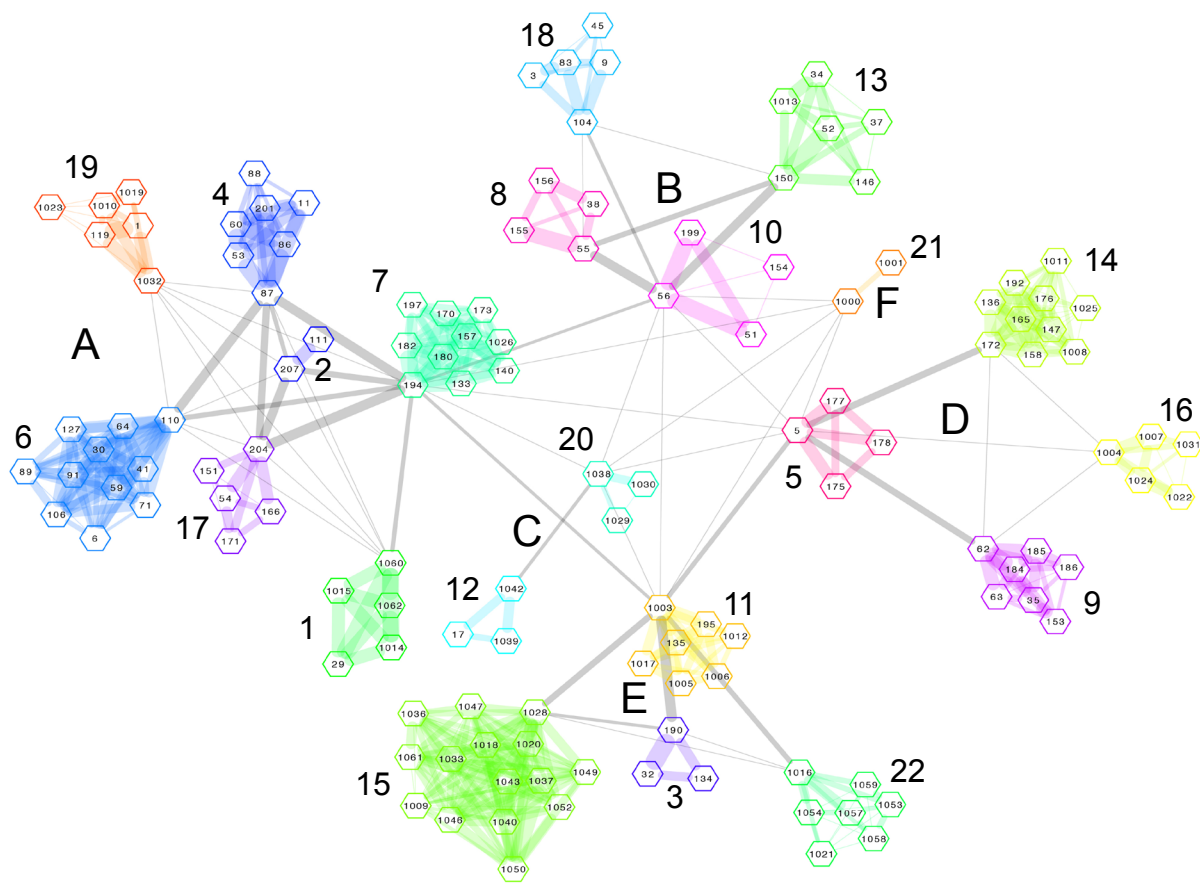
doi:10.1038/nature11005



Supplementary Figure 1: Screening format and curve-fitting algorithm. **a**, A schematic diagram of a typical 384-well screening plate. A single cell line is used on each plate and treated with 28 different drugs over a 9-pt, 256-fold concentration range. Wells with no cells (blanks) and untreated wells (controls) are used as controls on each plate. **b**, An example of curve-fitting of drug sensitivity data to generate a multi-parameter description of drug response. Red circles are normalized screening data and the curve fit is shown. Green circles represent IC₁₀, IC₂₅, IC₅₀, IC₇₅ and IC₉₀ values and error bars are confidence intervals. **c**, Representations of output parameters calculated from the curve-fitting algorithm. The slope parameter (beta) and IC₅₀ value from the dose-response curve are shown.



Supplementary Figure 2: Cell line sensitivity across the drug collection. Drugs are classified as clinically approved, clinically approved chemotherapeutics, in clinical development or experimental. For each drug the range of cell line IC_{50} values is represented as a box and whisker plot. The median IC_{50} , interquartile ranges, and 95% confidence intervals are shown for each drug. Outlier cell line IC_{50} s are indicated by black dots.



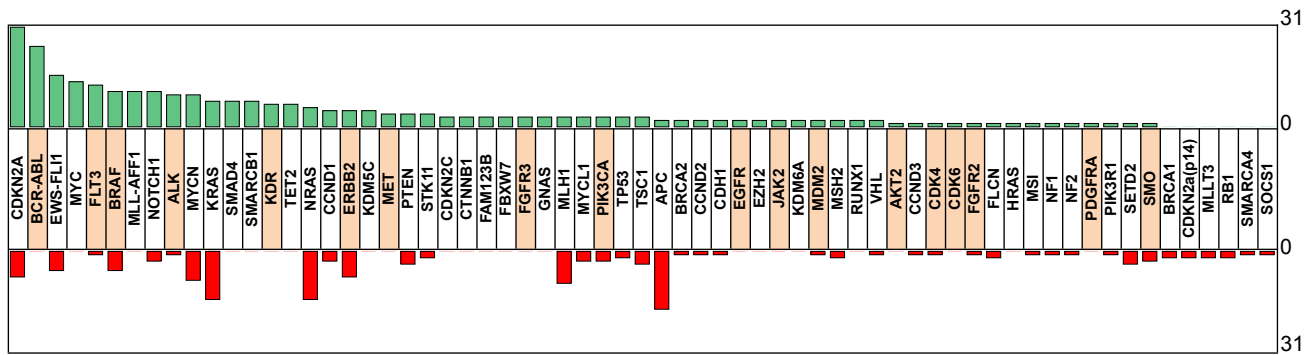
Supplementary Figure 3: Clustering of drugs based on IC_{50} values. A network visualization of drug similarity based on cell line IC_{50} values. Drugs are clustered in 22 communities (1-22) and 6 “communities of communities” (A-F, rich clubs) dependent on their intra and inter cluster correlations, respectively. An ID number identifies individual drugs and the thickness of an edge is proportional to the similarity of the connected nodes and different colors indicate different clusters. Node positions roughly reflect drug similarities (i.e. the closer two nodes are the more correlated the IC_{50} patterns of the corresponding drugs are) and have been computed through the “spring-embedding” algorithm for network layout.

C	total Avg Corr	odd Ratio	Drug id	Avg Corr	Drug Generic Name	Drug Target	C	total Avg Corr	odd Ratio	Drug id	Avg Corr	Drug Generic Name	Drug Target
1	0.7338	5.8277	1060	0.8162	PD-0325901 *	MEK1/2	13	0.4602	3.6161	150	0.6569	Bicalutamide *	Androgen receptor
			1062	0.7999	AZD6244	MEK1/2				52	0.6457	GNF-2	BCR-ABL
			1014	0.7961	RDEA119	MEK1/2				34	0.5551	Imatinib	ABL, KIT, PDGFR
			29	0.7644	AZ628	BRAF				1013	0.5312	Nilotinib	ABL
2	0.6960	5.5745	1015	0.7585	CI-1040	MEK1/2				146	0.4924	A-769662	AMPK
			207	0.8480	AS601245 *	JNK				37	0.4198	PF-2341066	MET, ALK
3	0.6600	5.1446	111	0.8480	Salubrinal	GADD34-PP1C phosphatase	14	0.4362	3.4325	172	0.5933	Embelin *	XIAP
			190	0.8164	Bleomycin *	DNA damage				147	0.5606	NSC-87877	SHP1/2
			32	0.8077	VX-680	Aurora A/B/C, FLT3, ABL1, JAK2,				165	0.5532	DMOG	Prolyl-4-Hydroxylase
4	0.6409	5.0275	134	0.6958	Etoposide	TOP2				176	0.5527	IPA-3	PAK
			87	0.7933	GW843682X *	PLK1				158	0.5477	PF-562271	FAK
			60	0.7861	Bi-2536	PLK1/2/3				136	0.5239	Mitomycin	DNA crosslinker
			86	0.7402	A-443654	AKT1/2/3				192	0.4787	LFM-A13	BTK
			201	0.7302	Epothilone B	Microtubules				1008	0.4575	Methotrexate	Dihydrofolate reductase (DHFR)
			53	0.7286	CGP-60474	CDK1/2/5/7/9				1011	0.3896	ABT-263	BCL2, BCL-XL, BCL-W
			11	0.6501	Paclitaxel	Microtubules				1025	0.2685	SB 216763	GSKa/b
			88	0.4169	MS-275	HDAC				1028	0.5844	VX-702 *	p38 MAPK
5	0.5500	4.3118	5	0.7202	Sunitinib *	PDGFRa, PDGFRb, KDR, KIT, FLT3	15	0.4296	3.3583	1043	0.5728	JNK Inhibitor VIII	JNK
			177	0.6586	GSK-650394	SGK3				1046	0.5212	681640	WEE1, CHK1
			175	0.6372	PAC-1	CASP3 activator				1037	0.5187	BX-795	TBK1, PDK1, IKK, AURKB/C
			178	0.6339	BAY 61-3606	SYK				1040	0.5150	BI-1870	RSK1/2/3/5/, PLK1, AURKB
6	0.5327	4.1633	110	0.6801	Roscovitine *	CDK5				1050	0.5146	ZM-447439	AURKB
			59	0.6578	WZ-1-84	BMX				1018	0.4974	ABT-888	PARP1/2
			91	0.6259	KIN001-135	IKKε				1061	0.4737	SB590885	RAF
			41	0.6087	S-Trityl-L-cysteine	KIF11				1020	0.4736	Lenalidomide	TNF alpha
			30	0.6008	Sorafenib	PDGFRa, PDGFRb, KDR, KIT, FLT3				1049	0.4250	PD-173074	FGFR1/3
			106	0.5917	XMD8-85	ERK5				1052	0.4221	RO-3306	CDK1
			64	0.5879	CMK	RSK				1036	0.4159	PLX4720	RAF
			127	0.5824	GSK269962A	ROCK				1047	0.3976	Nutlin-3a	MDM2
7	0.5266	4.1296	71	0.5208	Prymethamine	STAT3				1033	0.3718	GDC-0449	SMO
			89	0.4621	Parthenolide	NFκappaB				1009	0.3112	ATRA	Retinoic acid and retinoid X receptor agonist
			6	0.4089	PHA-685752	MET				1004	0.6108	Vinblastine *	Microtubules
			194	0.6685	NVP-AU922 *	HSP90				1024	0.5860	CEP-701	FLT3, JAK2, TrkA, RET
			180	0.6399	Thapsigargin	ATPase, Ca++ transporting, cardiac muscle, slow twitch 2				1007	0.5537	Doxetaxel	Microtubules
			157	0.6184	Obatoclax Mesylate	JNK				1022	0.5039	AZD7762	CHK1/2
			182	0.6082	Doxorubicin	BCL-2, BCL-XL, MCL-1				1031	0.4464	Elesclomol	HSP70
			133	0.5978	Vinorelbine	DNA intercalating				204	0.6454	Tipifarnib *	Farnesyl-transferase
8	0.5182	4.0438	140	0.5865	Shikonin	Microtubules				54	0.5818	CGP-082996	CDK4
			170	0.5530	FH535	unknown				171	0.5186	AKT inhibitor VIII	AKT1/2
			173	0.5296	Bryostatin 1	PRKC				151	0.4150	QS11	ARF GAP
			197	0.4869	17-AAG	HSP90				104	0.6076	Bortezomib *	Proteasome
			1026	0.4505	Retinoic acid X family agonist	SRC family				83	0.6004	JW-7-52-1	MTOR
			55	0.6868	A-770041 *	ABL				9	0.5175	Rapamycin	MTOR
			155	0.6437	AP-24534	PI3Kb				45	0.3952	Z-LNNle-CHO	Proteasome g-secretase
			156	0.6259	AZD6482	SRC, ABL				1032	0.5838	BIBW2992 *	EGFR, ERBB2
9	0.5055	3.9489	38	0.5982	AZD-0530	IGF1R	19	0.3659	2.8674	1	0.5620	Erlotinib	EGFR
			62	0.6946	BMS-536924 *	IGF1R				119	0.5479	Lapatinib	EGFR, ERBB2
			184	0.6846	BMS-754807	IGF1R				1010	0.4803	Gefitinib	EGFR
			35	0.6378	NVP-TAE684	ALK				1019	0.4036	Bosutinib	SRC, ABL, TEC
			153	0.5137	Midostaurin	KIT				1023	0.2519	GW 441756	NTRK1
			63	0.4895	BMS-509744	ITK				1038	0.6160	NU-7441 *	DNAPK
			186	0.4296	Bexarotene	Retinoic acid X family agonist				1030	0.5744	KU-55933	ATM
			56	0.7207	WH-4-023 *	SRC family				1029	0.5206	AMG-706	VEGFR, RET, c-KIT, PDGFR
10	0.4931	3.8986	51	0.6816	Dasatinib	ABL, SRC, KIT, PDGFR	20	0.3555	2.7617	1000	0.6733	Metformin *	AMPK
			199	0.6571	Pazopanib	VEGFR, PDGFRa, PDGFRb, KIT				1001	0.6733	AI CAR	AMPK
			154	0.4200	CHIR-99021	GSK3b				1016	0.4957	Temirosilimus *	mTOR
			1003	0.6594	Camptothecin *	TOP1				1057	0.4629	NVP-BEZ235	PI3K Class 1 and mTORC1/2
			195	0.6083	Camptothecin	TOP1				1053	0.3970	MK-2206	AKT1/2
			135	0.5947	Gemcitabine	DNA replication				1054	0.3943	PD-0332991	CDK4/6
			1006	0.5309	Cytarabine	Inhibits DNA synthesis				1058	0.3583	GDC0941	PI3K class 1
			1017	0.5292	AZD-2281	PARP1/2				1059	0.3444	AZD8055	mTORC1/2
11	0.4826	3.7883	1005	0.5141	Cisplatin	DNA crosslinking	22	0.2936	2.2959	1021	0.3093	Axitinib	PDGFR, KIT, VEGFR
			1012	0.4587	Vorinostat	HDAC inhibitor Class I, IIa, IIb, IV				1042	0.6823	p38, JNK2	* community exemplars
			1042	0.6823	BIRB 0796 *	p38, JNK2				1039	0.6489	RSK, AURKB, PIM3	
			17	0.6364	Cyclopamine	SMO				1039	0.6489	SL 0101-1	

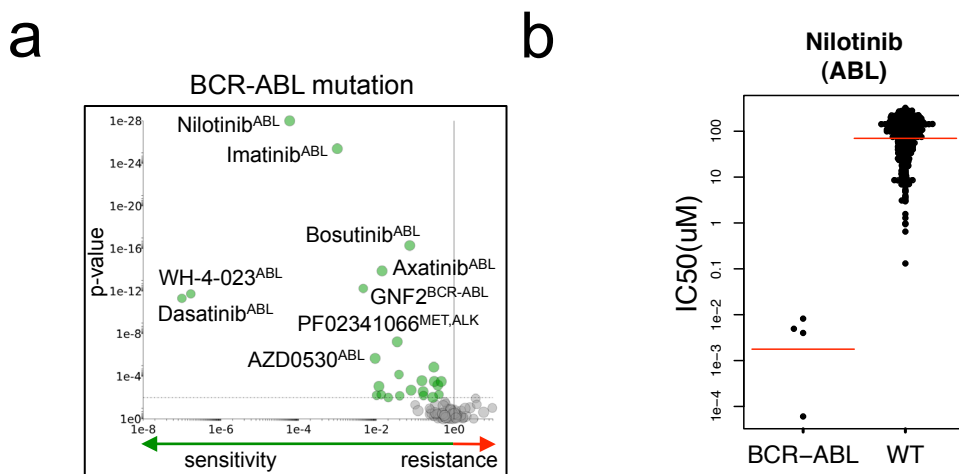
Supplementary Table 1: Intra-cluster drug correlations. Communities are sorted according to the intra-community similarity score and drugs are sorted according to their similarity to the exemplar (*) within each community. The intra-community similarity score is calculated as an odds ratio (see Supplementary Methods for more detail). As an experimental control the drug camptothecin was screened twice across the cell line collection and the resulting drug sensitivity data were correlative with both datasets clustering together in community 11 (C11). Drugs with overlapping reported targets such as multiple MEK1/2 (C1), EGFR/ERBB2 (C19) and IGFR1 (C9) inhibitors frequently clustered together demonstrating overlapping sensitivity profiles across the cell line panel. In some instances however this was not the case (e.g. SRC inhibitors, C8, C10 and C19) indicating perhaps differences in the modes of action and target selectivity of these drugs. The community clusters (C) correspond to the numbering in Supplementary Figure 3.

	1	2	4	6	7	17	19	8	10	13	18	12	20	5	9	14	16	3	11	15	22	21
1				0.2395	0.3477									-0.8813	-0.1916						-0.1384	
2				0.2643		0.2544	0.2856															
4				0.3428	0.4440	0.4665		0.2756						0.3422							A	
6	0.2395		0.3428	0.3112	0.2756			0.2434	-0.1268		-0.2788			-0.9193	0.2385	-0.2777						
7	0.3477	0.2544	0.4440	0.3112	0.3194			0.2657						-0.5656	0.2349	-0.3827					-0.1291	
17		0.2856	0.4665	0.2756	0.3194			0.2778		-0.5179	-0.1130			-0.4989	-0.2494	-0.3555						
19									0.4260	0.2723						-0.1537					-0.5998	
8		0.2756	0.2434	0.2657	0.2778			0.4260	0.2723													
10				-0.1268		-0.5179		0.4260	0.2947	0.2415												
13								0.2723	0.2947													
18				-0.2788		-0.1130		0.2415													-0.1468	
12												0.2812										
20								0.2812														
5	-0.8813			-0.9193	-0.5656		-0.4989							0.2664	0.4177		0.3689	0.3544				
9				0.3163	0.2385	0.2349	-0.2494							0.2664			0.2365				-0.2956	
14	0.1916			-0.9376	-0.2777	-0.3827	-0.6515	-0.3555	-0.1537					0.4177			0.1990				0.3117	
16																	0.2698	-0.6500	0.2296			
3		0.3422	0.3928		0.3265	0.3382								0.3689			0.4197					
11				0.2496	-0.1778		-0.1846							0.3544	0.2365	0.1990	0.2698	0.4197	0.2762	-0.3716		
15					-0.4549											-0.6500		0.2296				
22																	-0.2956	0.3117				
21	-0.1384			-0.1291			-0.5998		-0.1468													
	A	B	C	D	E	F																

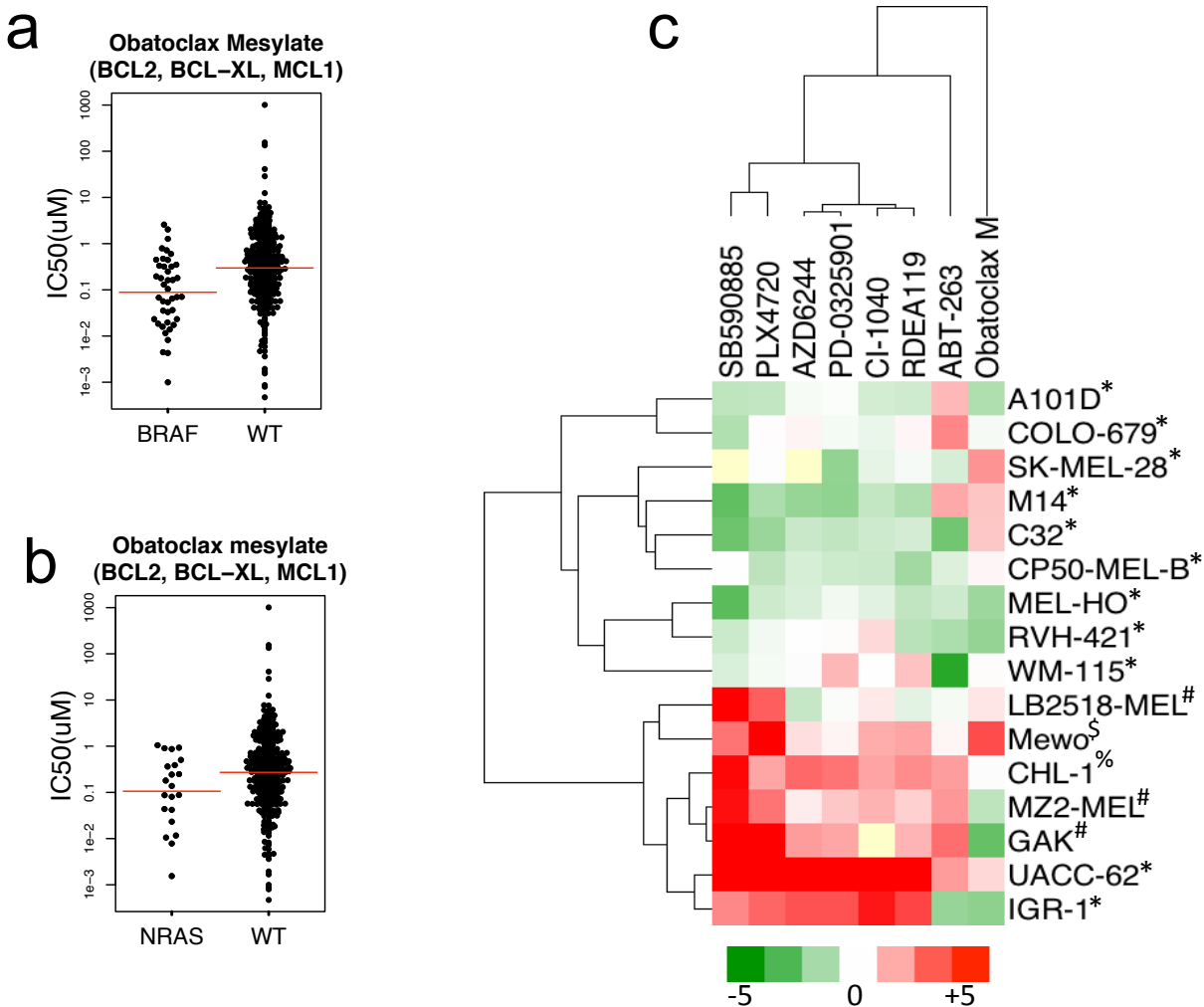
Supplementary Table 2: Cluster-to-cluster similarity scores and rich-club compositions. The inter-cluster similarity score is provided for each pair of communities and quantifies the extent of their similarity. Green values indicates positive similarities (correlations) while red values indicate "negative" ones (anti-correlations). Only significant values ($P < 0.05$) were included and communities (1 - 22) were grouped to reflect the rich-club compositions (A - F).



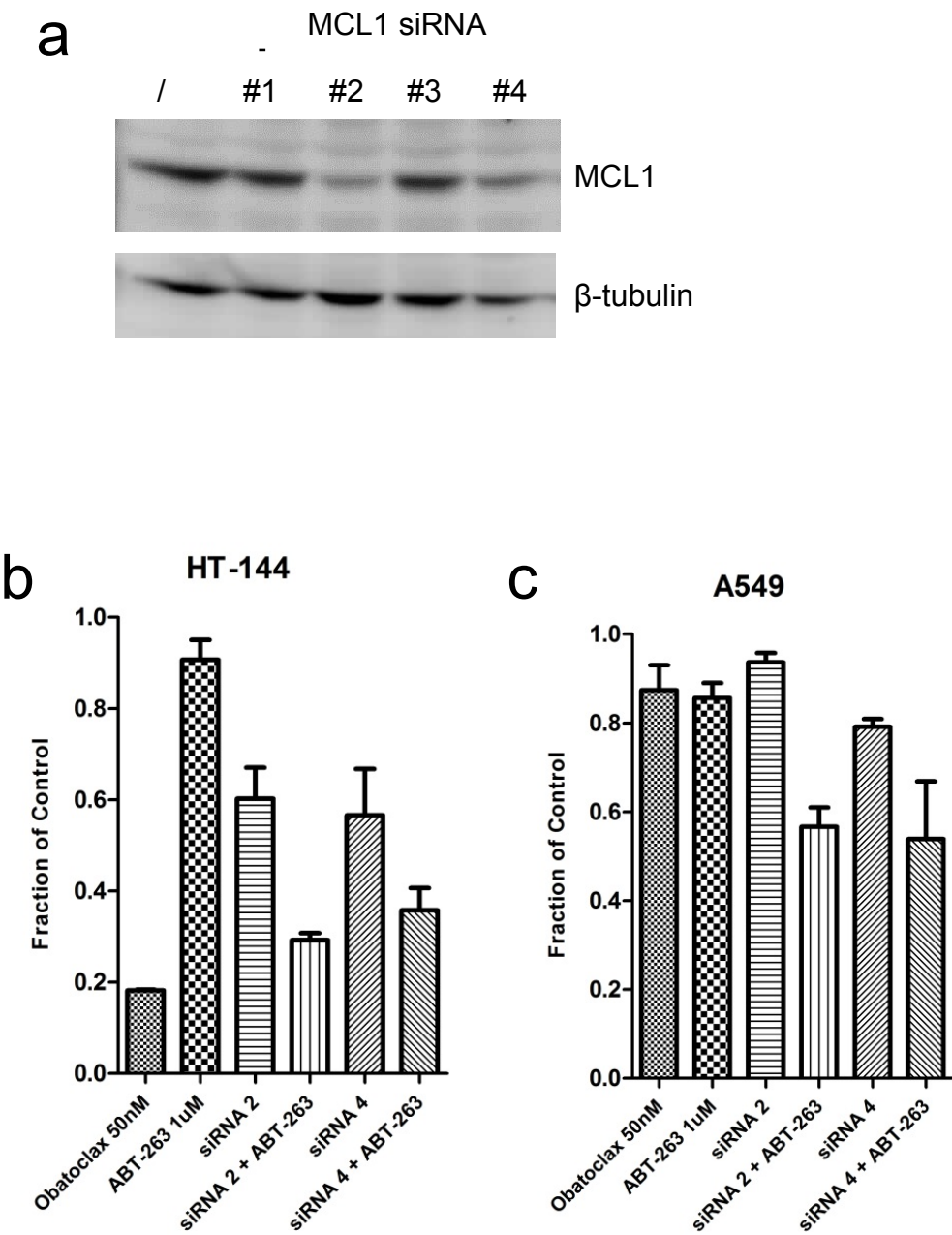
Supplementary Figure 4: The majority of cancer genes are associated with drug response. The number of statistically significant sensitizing (green bars) or resistance (red bars) associations identified by MANOVA for each cancer gene. Genes that are reported to be the direct target of a screening drug are coloured. The following genes were analysed but were not associated with drug response: *IDH1*, *MAP2K4*, *KIT*, *MSH6*. Drug response was also correlated with microsatellite instability (MSI) status.



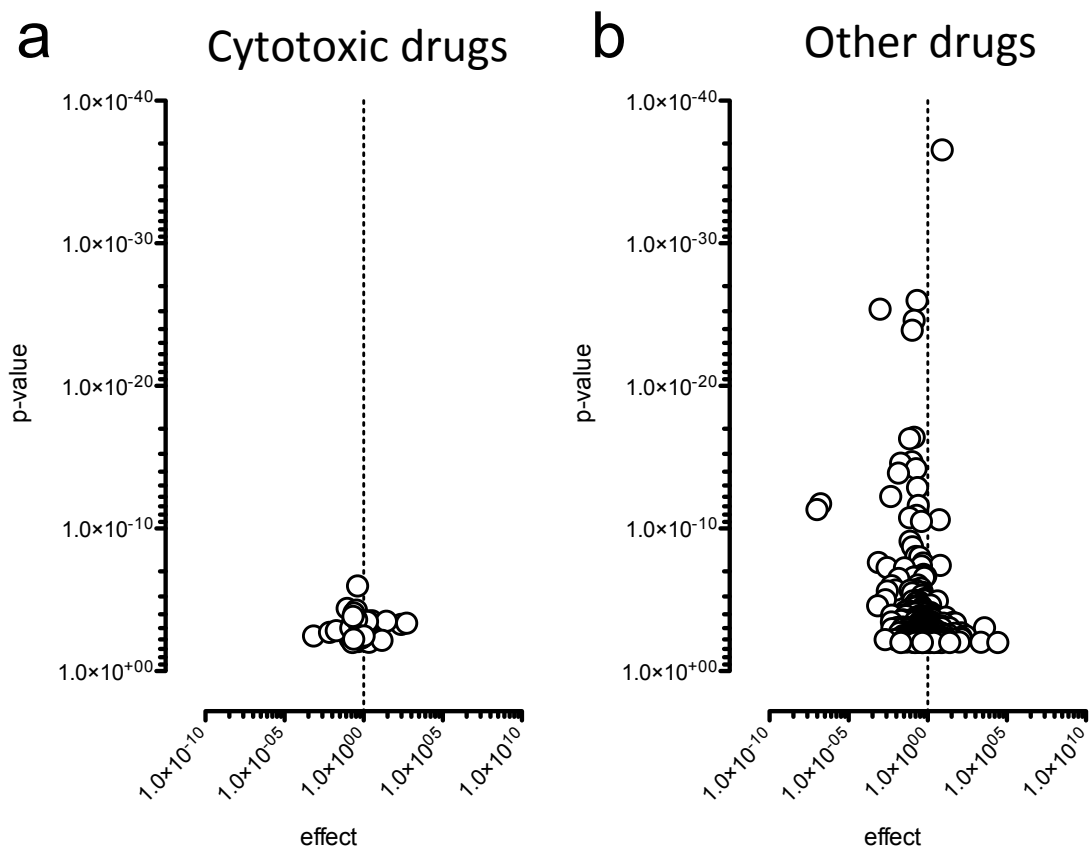
Supplementary Figure 5: The *BCR-ABL* rearrangement is associated with sensitivity to multiple ABL inhibitors. **a**, A gene-specific volcano plot from the MANOVA showing the magnitude (effect; x-axis) and significance (p-value; inverted y-axis) of drug sensitivity associated with *BCR-ABL* mutations in cancer cell lines. Each circle represents a single drug interaction and for selected associations the drug name and therapeutic drug target(s) (in superscript) are indicated. A horizontal dashed line indicates the threshold of statistical significance (0.2 FDR, $P < 0.0099$) and significant associations with drug sensitivity are coloured green. *BCR-ABL* was not associated with drug resistance. For clarity, the p-value for nilotinib ($P = 2.54 \times 10^{-65}$) has been capped at 1×10^{-28} . **b**, A scatter plot of *BCR-ABL* mutated or wild-type (WT) cell line IC₅₀ values for nilotinib. Each circle represents the IC₅₀ of one cell line on a log scale and the red bar is the geometric mean.



Supplementary Figure 6: BRAF and NRAS mutations are markers of melanoma sensitivity to obatoclax mesylate. **a** and **b**, Scatter plots from screening data of obatoclax mesylate IC₅₀ values of **a**, BRAF or **b**, NRAS mutated versus wild-type (WT) cell lines. The p-values from the MANOVA analysis for these associations are $P = 1.4 \times 10^{-4}$ and $P = 0.0055$ for BRAF and NRAS, respectively. Each circle represents the IC₅₀ of one cell line on a log scale and the red bar is the geometric mean. **c**, A heatmap comparing sensitivity of melanoma cell lines to obatoclax mesylate, ABT-263, BRAF inhibitors (PLX4720, SB590885), MEK1/2 inhibitors (AZD6244, PD-0325901, CI-1040, RDEA119). Sensitivity to obatoclax is not correlated with sensitivity to MEK or BRAF inhibitors. The colour scale corresponds to median centered natural log (IC₅₀) values. Mutational status is indicated as follows: *, BRAF V600; #, NRAS; \$, NF1; %, KRAS amplified.

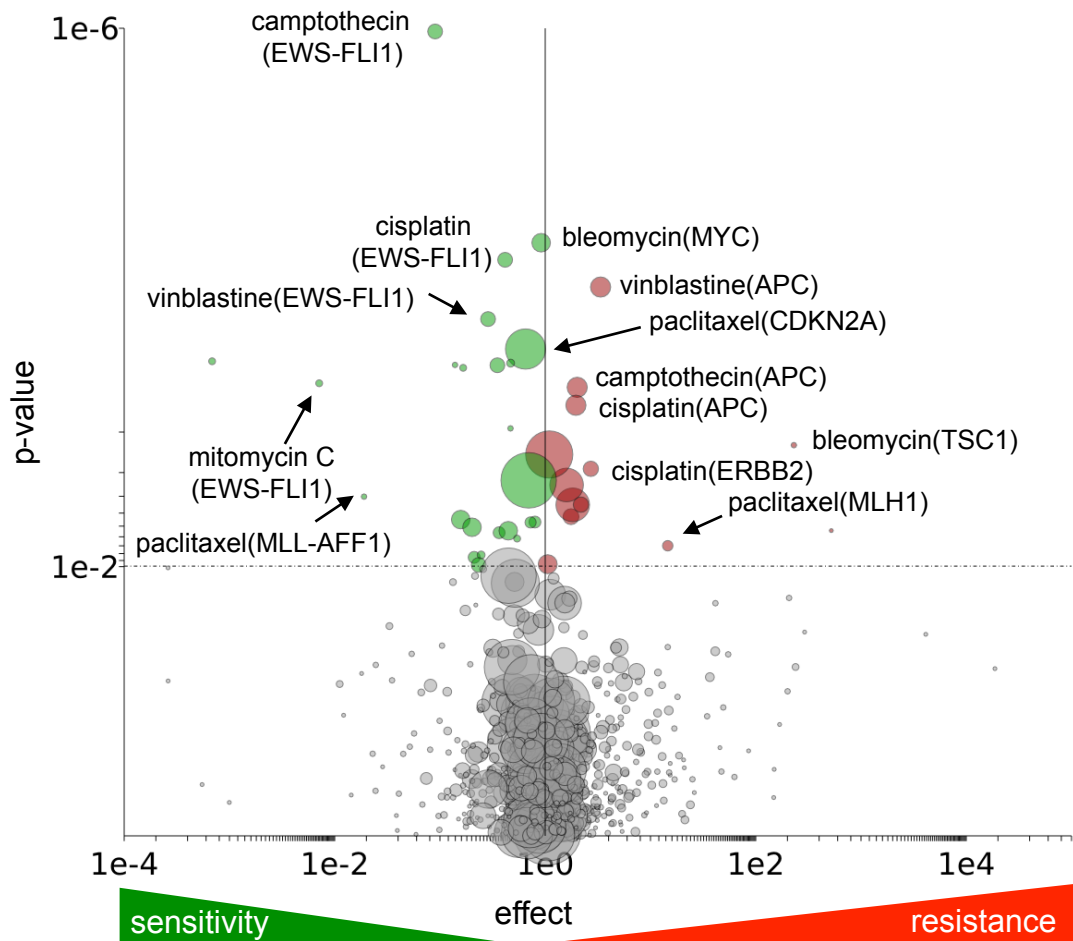


Supplementary Figure 7: MCL1 knockdown sensitises melanoma cells to ABT-263. **a**, Western blot of MCL1 protein levels in mock transfected cells or following 72 hr knockdown with multiple MCL1 siRNA. siRNA #2 and #4 gave the most efficient knockdown and were selected for subsequent cell viability assays. **b** and **c**, Effect on the cell viability of the *BRAF* (V600E) mutant HT-144 melanoma cell line after 72 hour treatment with obatoclax (50 nM), or ABT-263 (1 μM) alone or together with 40 nM MCL1 siRNA. The lung cancer cell line A549 which is wild-type for *BRAF* was used as negative control. Cell viability was assayed in triplicate and error bars represent standard deviations.



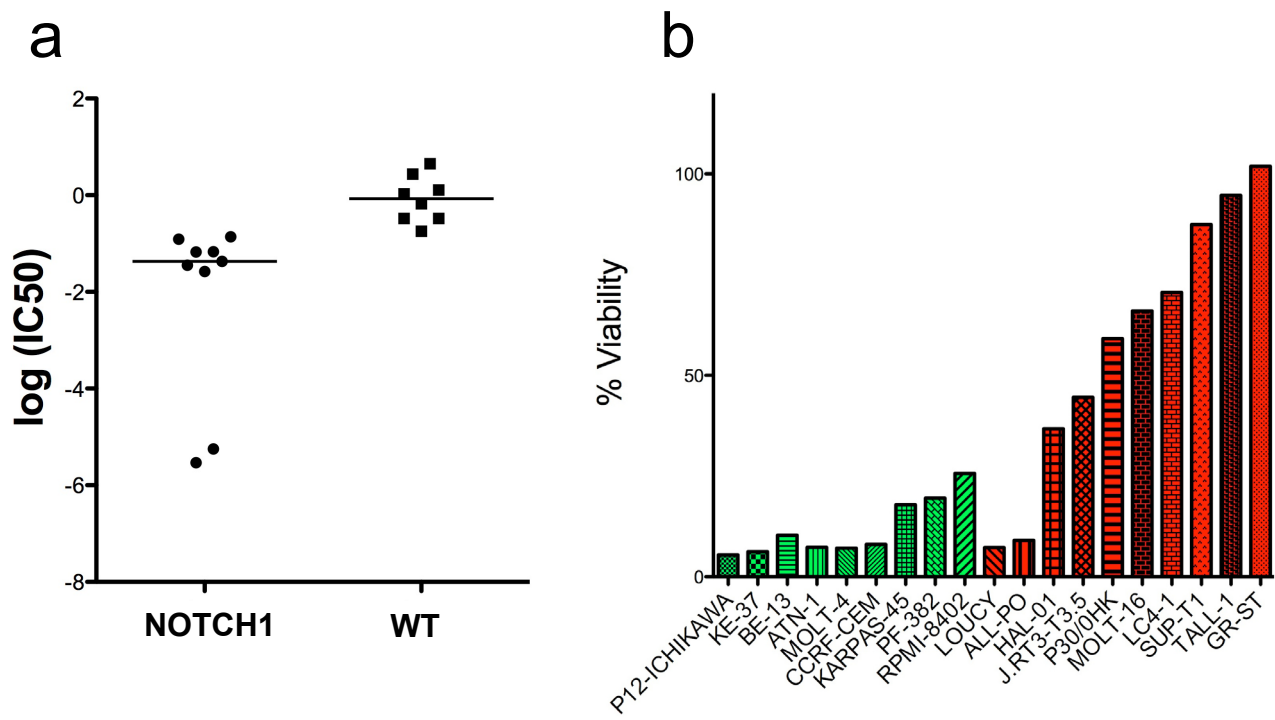
Supplementary Figure 8: Cytotoxic chemotherapeutic drugs were not associated with highly significant genomic correlations. Volcano plots showing the effect size (x-axis) and p-value (y-axis, inverted scale) of statistically significant associations identified by the MANOVA. **a**, Cytotoxic drugs ($n=13$) were correlated with 41 associations and **b** the remaining drugs ($n=117$) with 407 associations. For clarity the association between nilotinib and *BCR-ABL* ($P = 2.45 \times 10^{-65}$) has been excluded from **b**.

Cytotoxic drugs

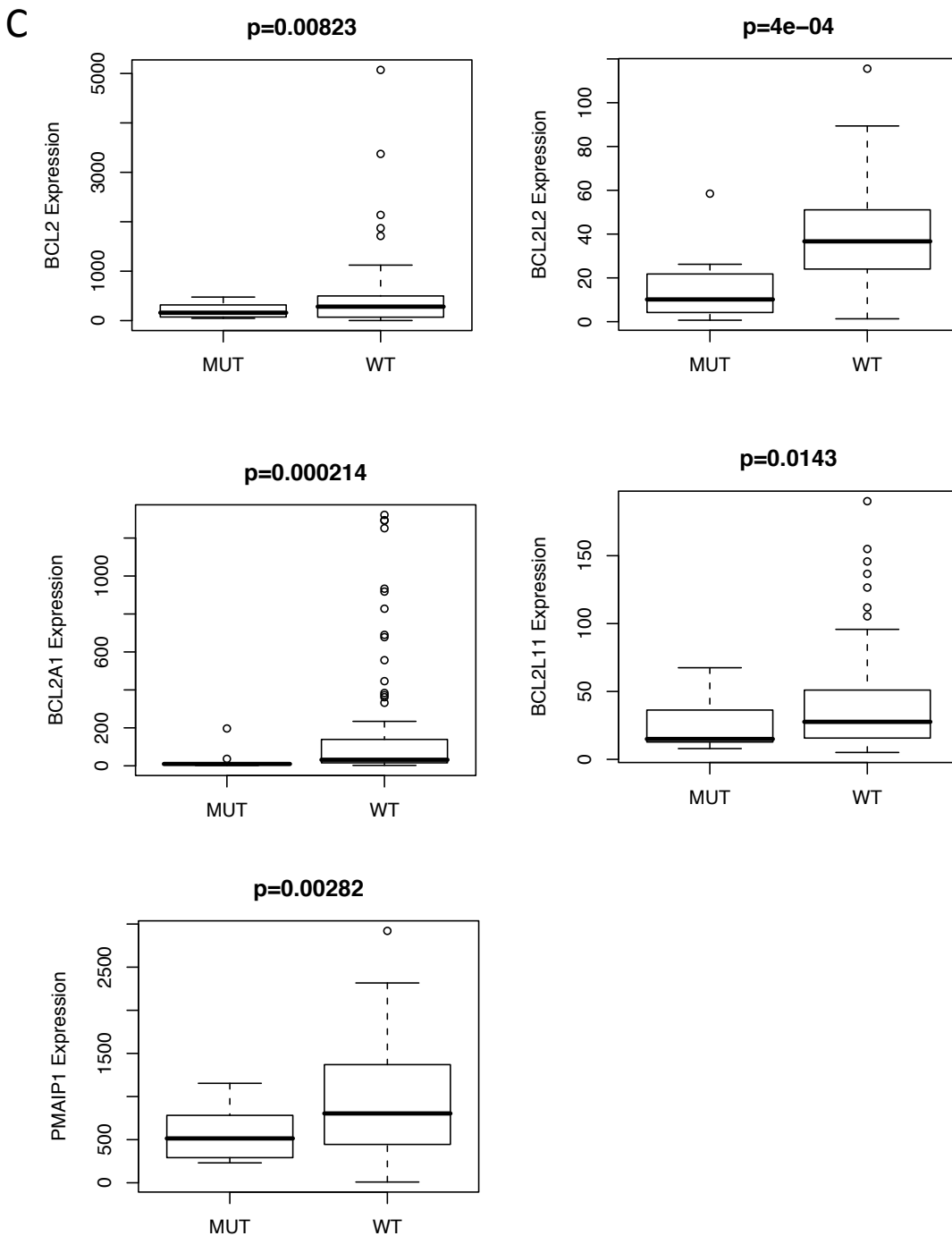


Supplementary Figure 9: Genomic markers of sensitivity to cytotoxic chemotherapeutics.

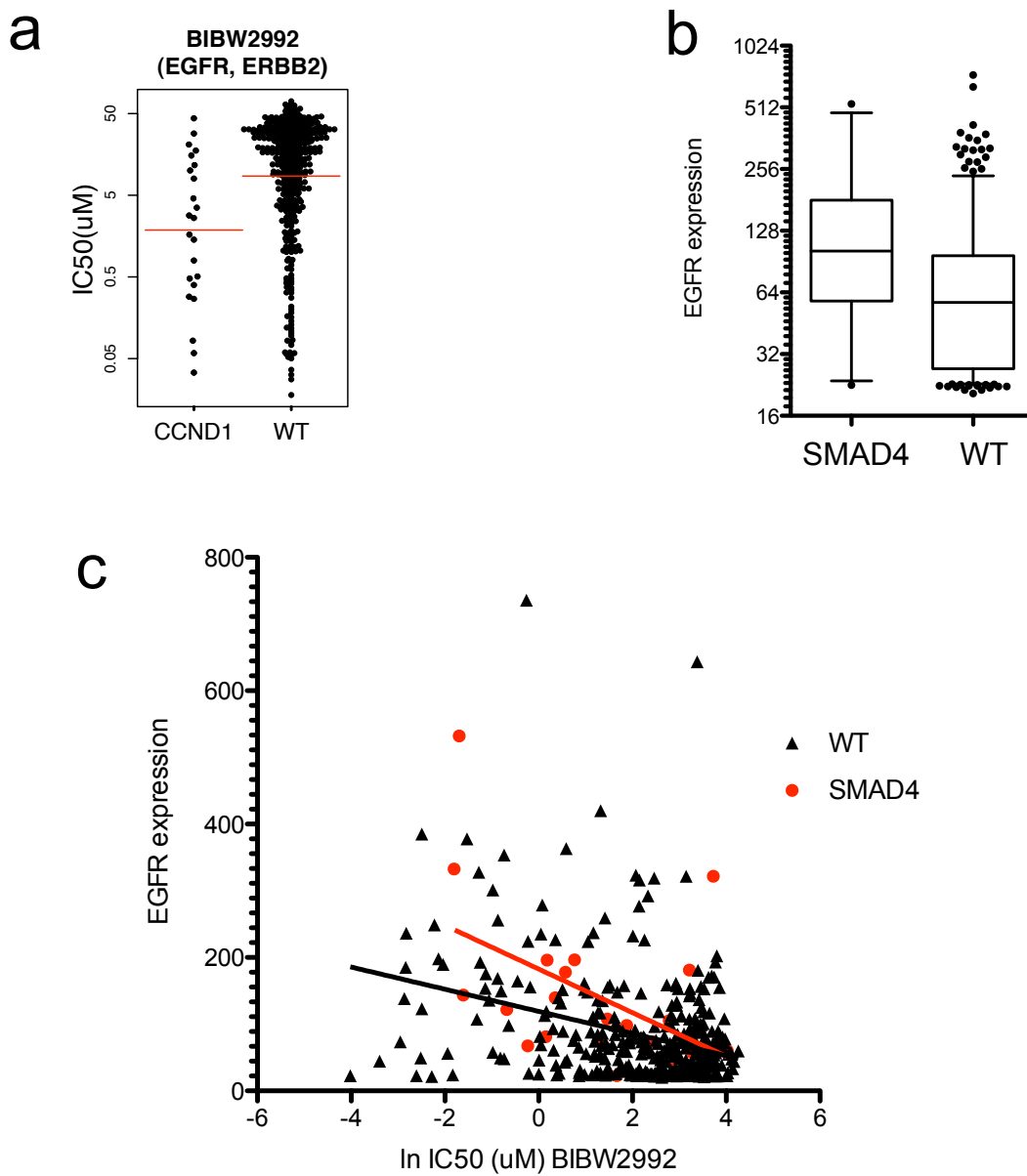
A volcano plot representation of cytotoxic drugs ($n = 13$ drugs) from the MANOVA showing the magnitude (effect; x-axis) and significance (p-value; inverted y-axis) of all drug-gene associations. Each circle represents a single drug-gene interaction and the circle size is proportional to the number of mutant cell lines screened (maximum = 312). The horizontal dashed line indicates the threshold of statistical significance (0.2 FDR, $P < 0.0099$) and significant associations with drug sensitivity or resistance are coloured green and red, respectively. Select significant drug-gene associations are labeled with drug name and gene name (bracketed).



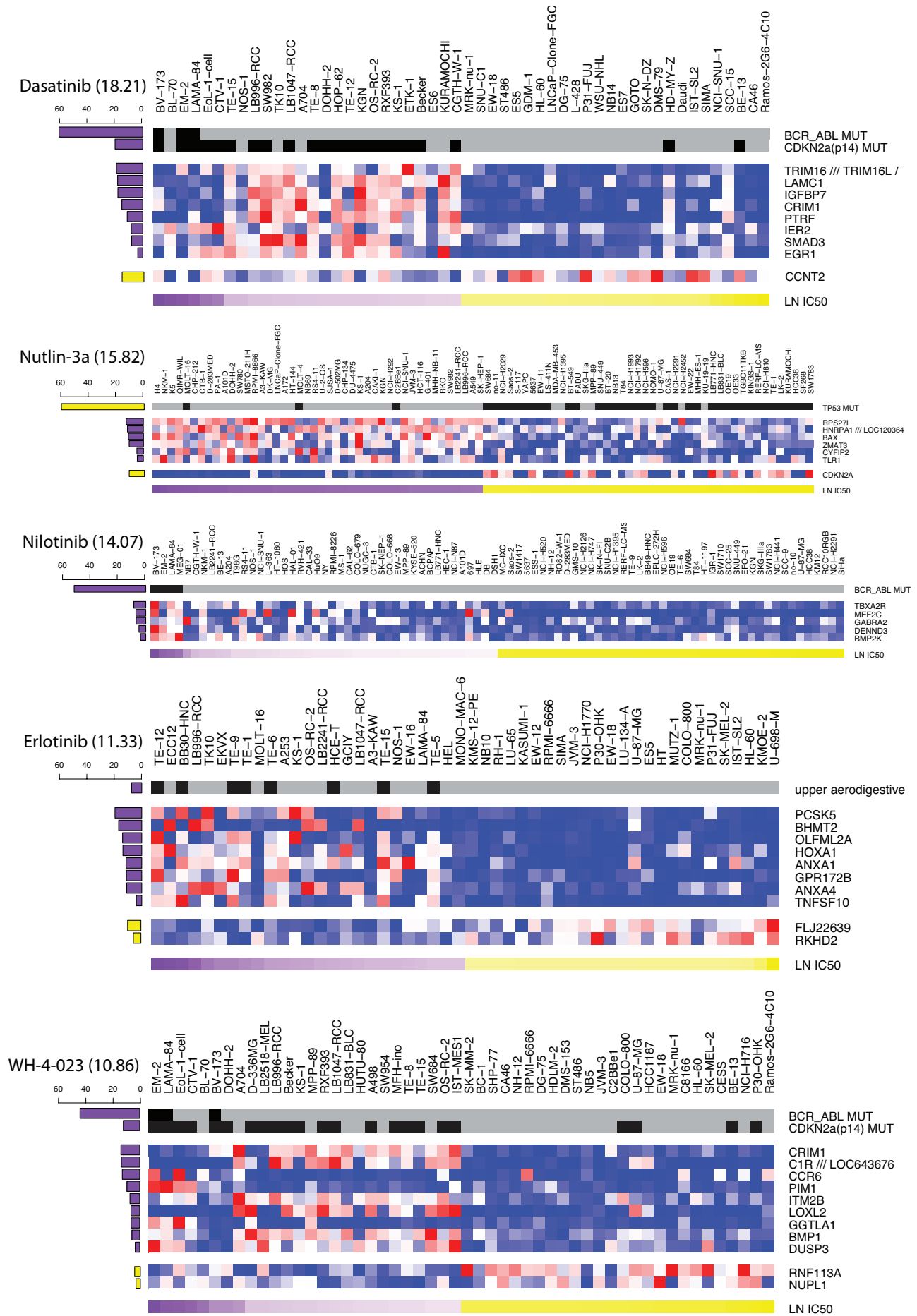
Supplementary Figure 10: Sensitivity of NOTCH1 mutant leukemic cell lines to ABT-263 following 7 day drug treatment. A panel of leukemic lines (9 NOTCH1 mutant and 8 wild-type) were treated for 7 days with increasing concentrations of ABT-263 (40 nM – 10 uM). **a**, The concentration of ABT-263 necessary to obtain 50% reduction in cell number (IC₅₀) was determined to be significantly lower for NOTCH1 mutant lines ($P < 0.0001$, student t-test) than wild-type (WT) lines. **b**, Normalised cell viability following 7 days of treatment with 0.31 uM ABT-263 for NOTCH1 mutant (green fill, $n = 9$) and wild-type (red fill, $n = 10$) cell lines.

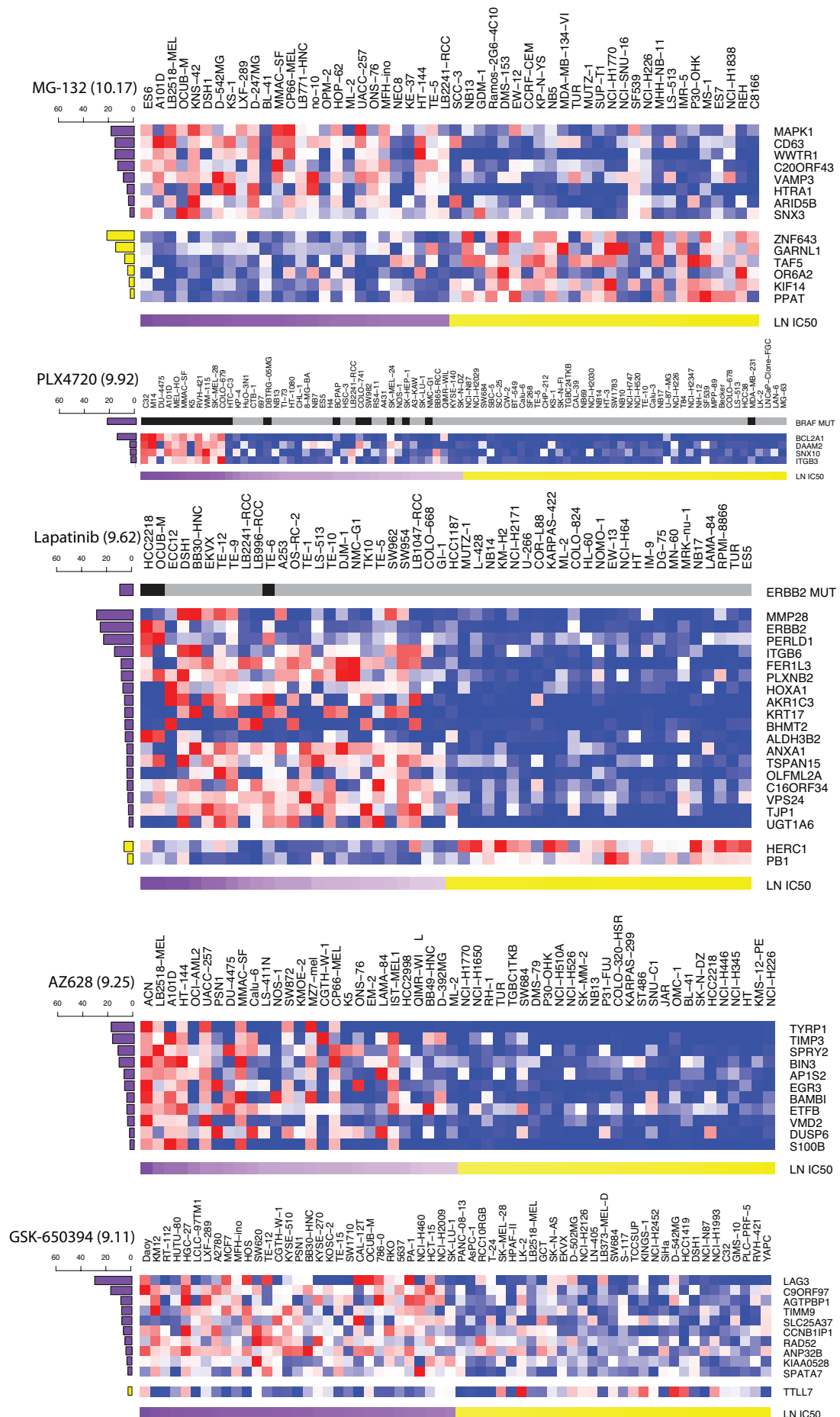


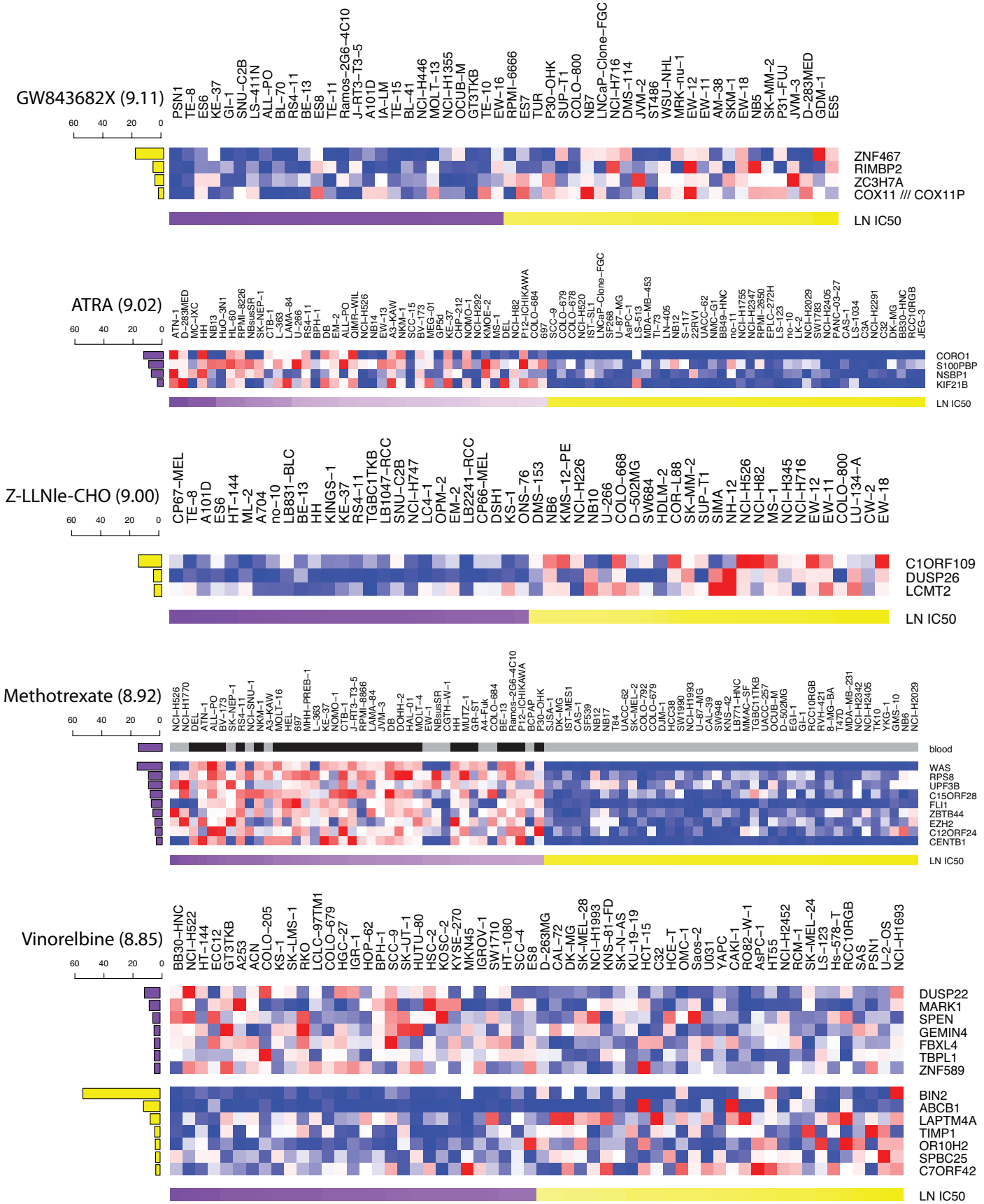
Supplementary Figure 11: Decreased expression of apoptotic genes in *NOTCH1* mutant compared to wild-type hematopoietic cell. Expression levels of the indicated genes were obtained from the U133A microarray dataset and statistical significance tested using student t-test. *NOTCH1* is frequently mutated in hematopoietic cell lines and so only cell lines of hematopoietic origin were considered to minimize tissue specific effects on expression (*NOTCH1* (MUT), $n = 12$; wild-type (WT), $n = 80$). Additional apoptotic regulators tested were not differentially expressed (*BAD*, *BBC3*, *BCL2L10*, *BID*, *BIK*, *BNIP1*, *BNIP2*, *BNIP3*, *MCL1*).

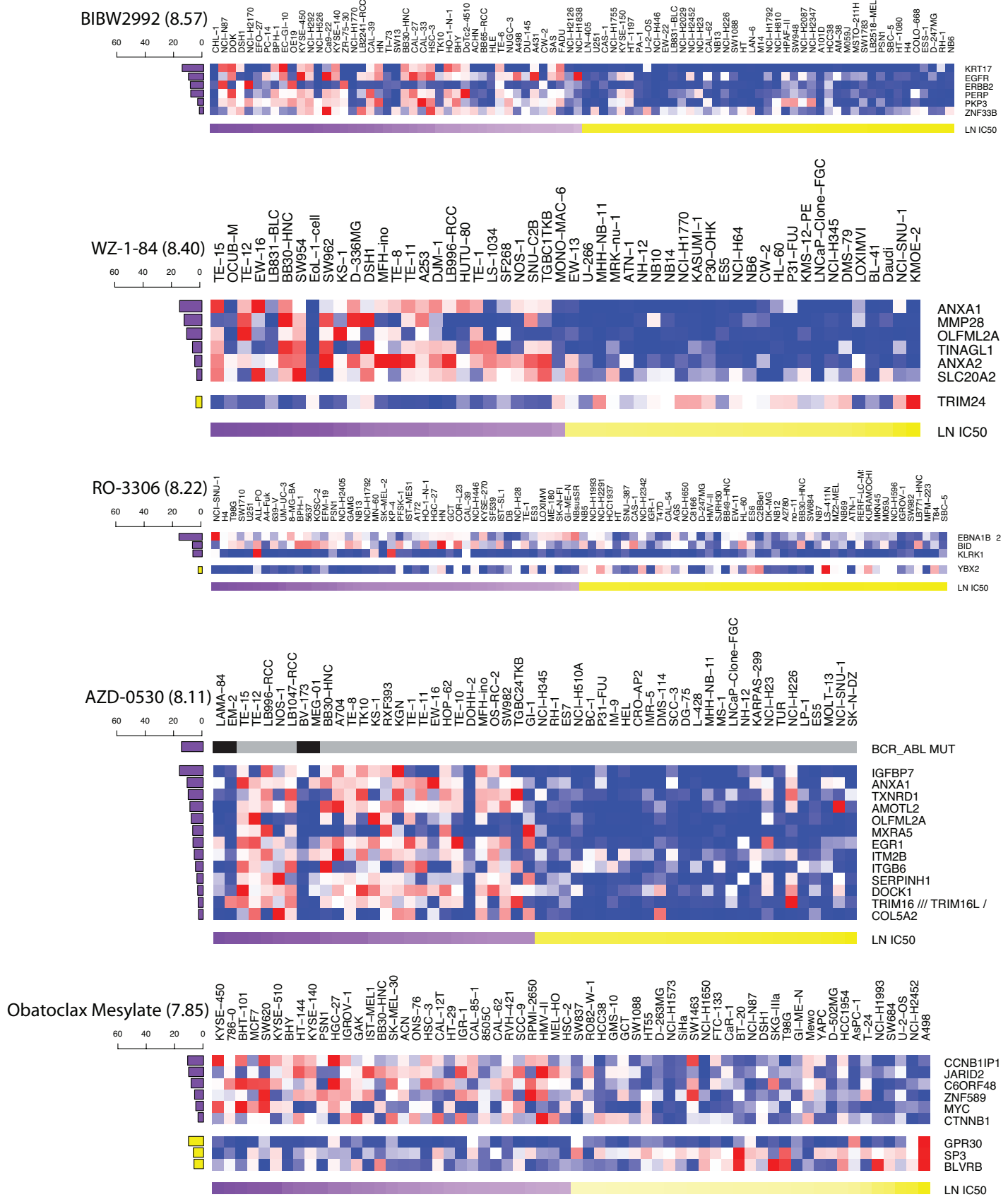


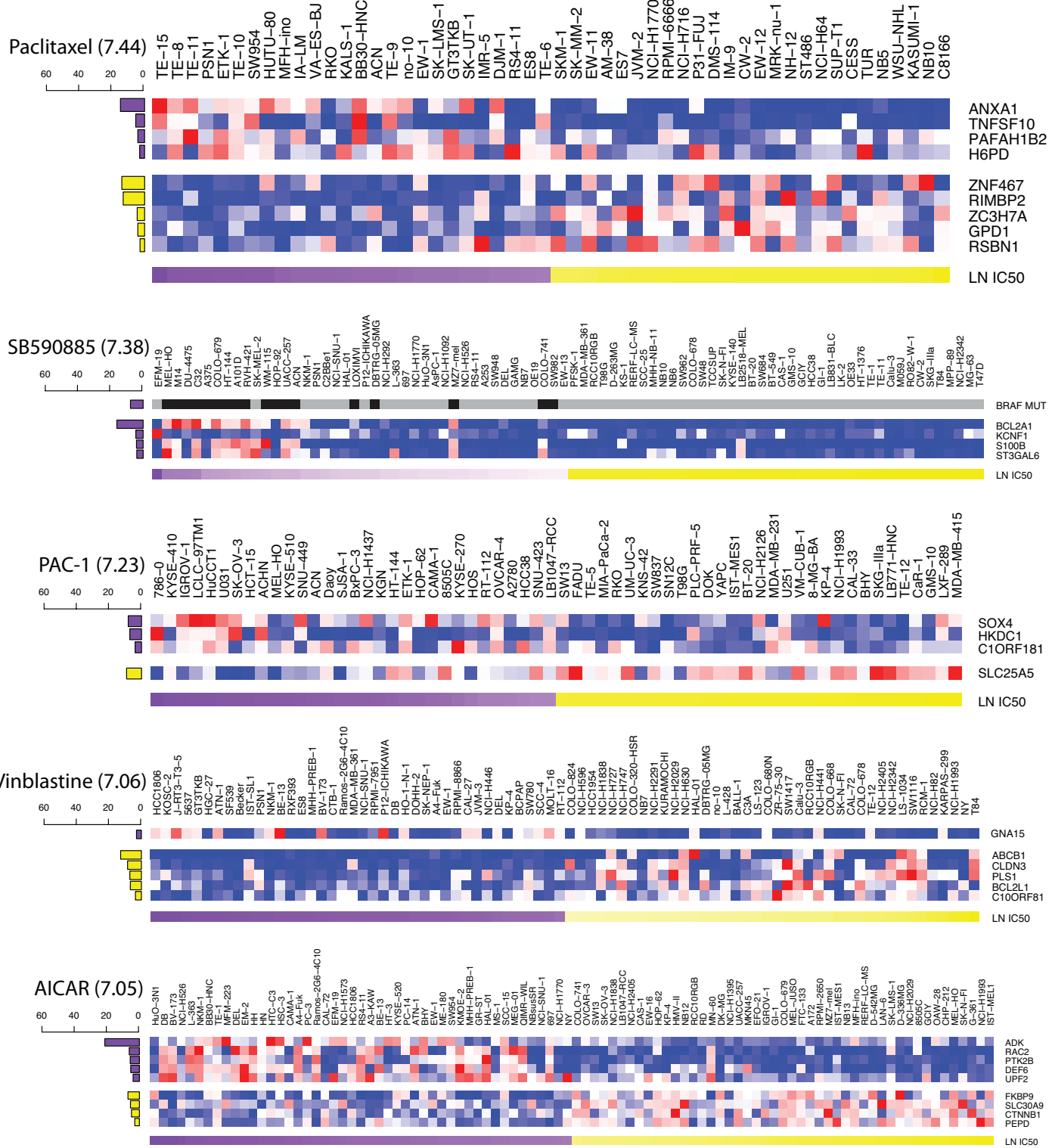
Supplementary Figure 12: Sensitivity of SMAD4 mutated cell lines to EGFR inhibitors is associated with increased EGFR expression. **a**, A scatter plot of *CCND1* mutated or wild-type (WT) cell line IC₅₀ values for BIBW2992 ($P = 6.7 \times 10^{-4}$ from the MANOVA). Each circle represents the IC₅₀ of one cell line on a log scale and the red line is the geometric mean. **b**, *EGFR* gene expression is elevated in SMAD4 mutated cell lines ($P = 0.0031$, students t-test). A box and whisker plots of gene expression levels in wild-type (WT, $n = 399$) cell lines or cell lines with a SMAD4 mutation ($n = 24$). Whiskers indicate the 5th and 95th percentiles and outlier cell lines are indicated by black dots. Cell lines with *CCND1* mutation were also correlated with sensitivity to EGFR inhibitors from the MANOVA analysis but where not associated with altered *EGFR* gene expression. **c**, Cell line sensitivity to EGFR/ERBB2 inhibitor BIBW2992 is correlated with *EGFR* expression levels in WT (spearman correlation, $r = -0.2051$, $P < 0.0001$, $n = 399$) and SMAD4 mutated ($r = -0.5313$, $P = 0.0075$, $n = 24$) cell lines. Linear regressions for WT (black line) and SMAD4 mutated (red line) cell lines are shown. For the analysis in **b** and **c** all *EGFR* or *ERBB2* mutated cell lines were excluded.

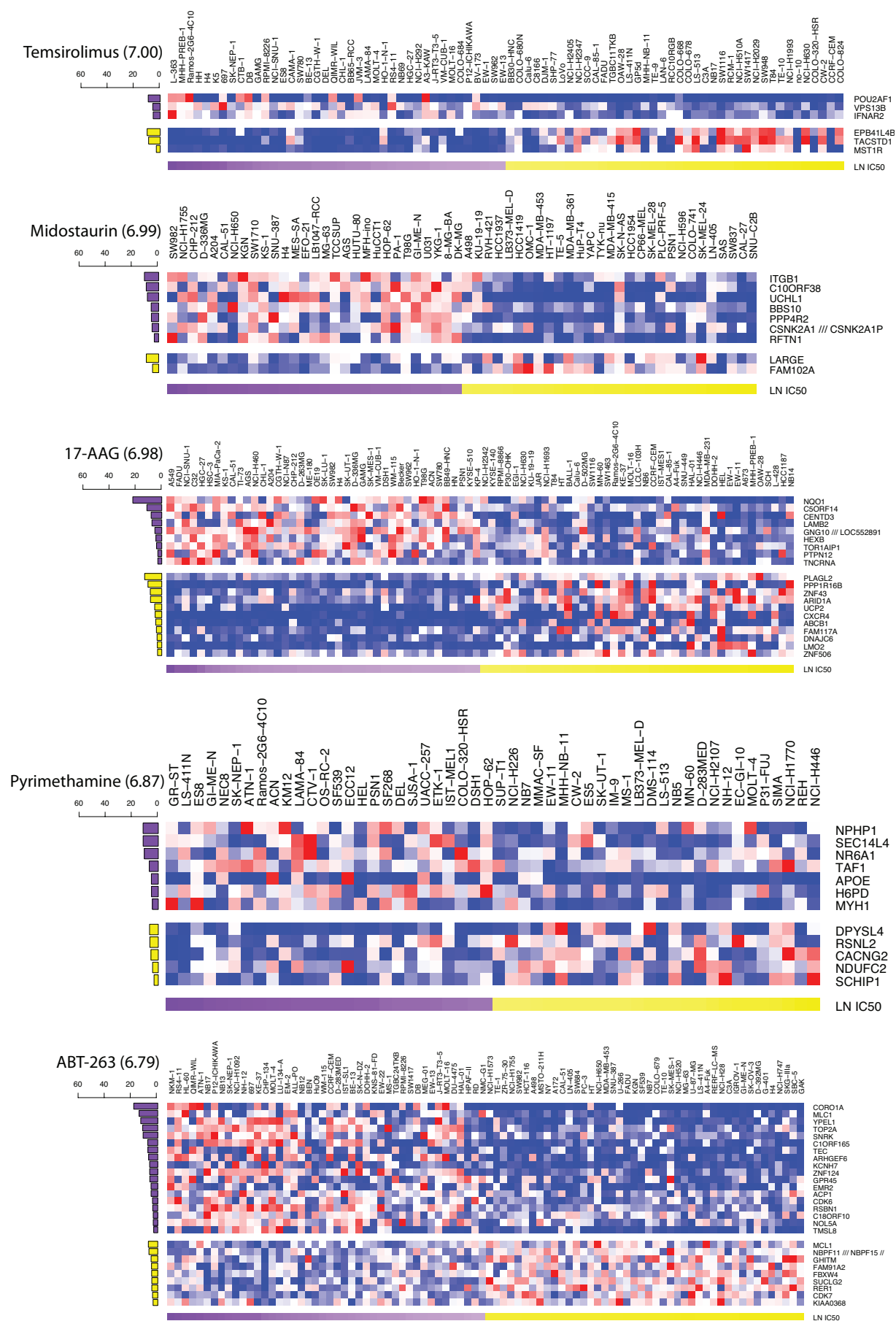


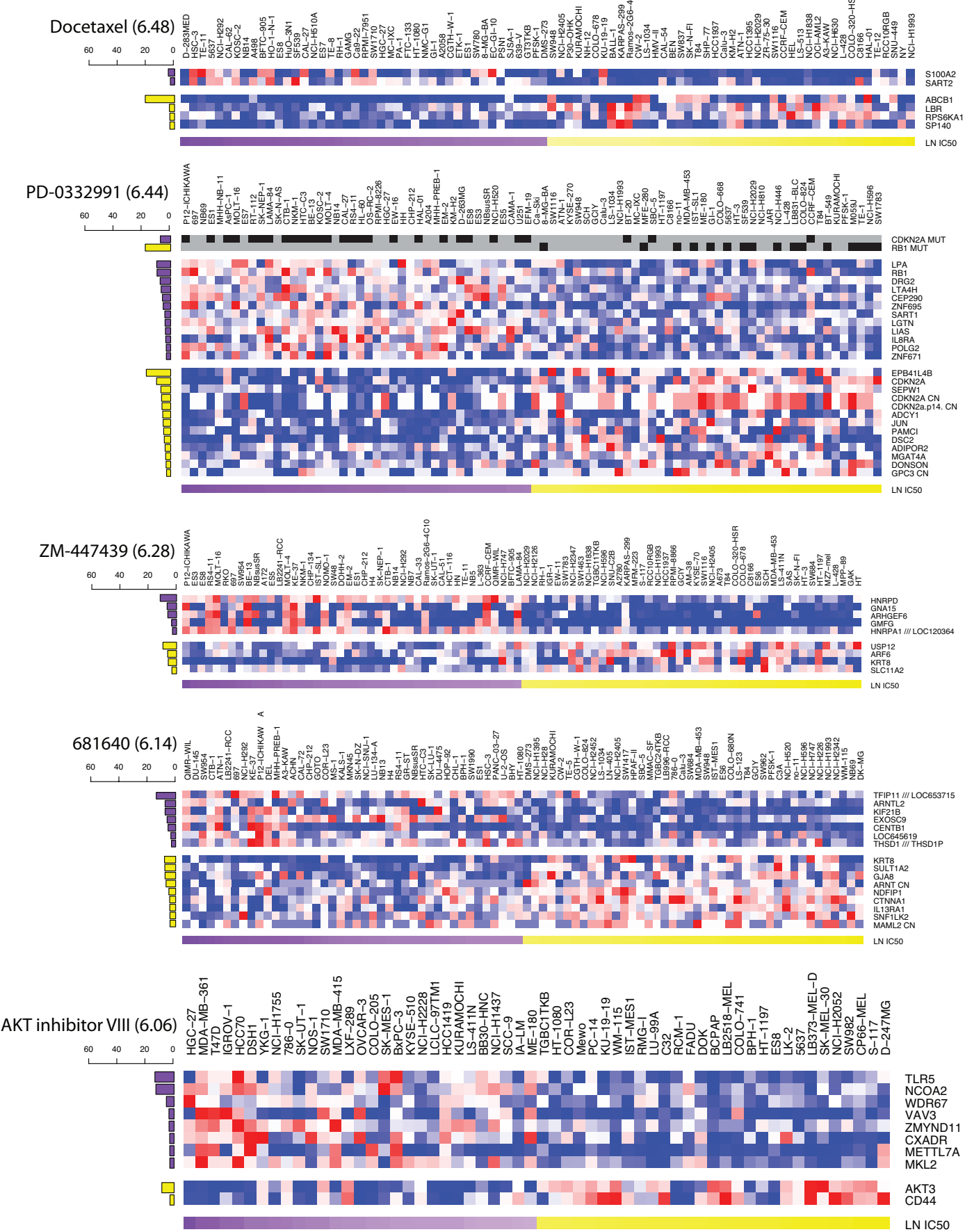


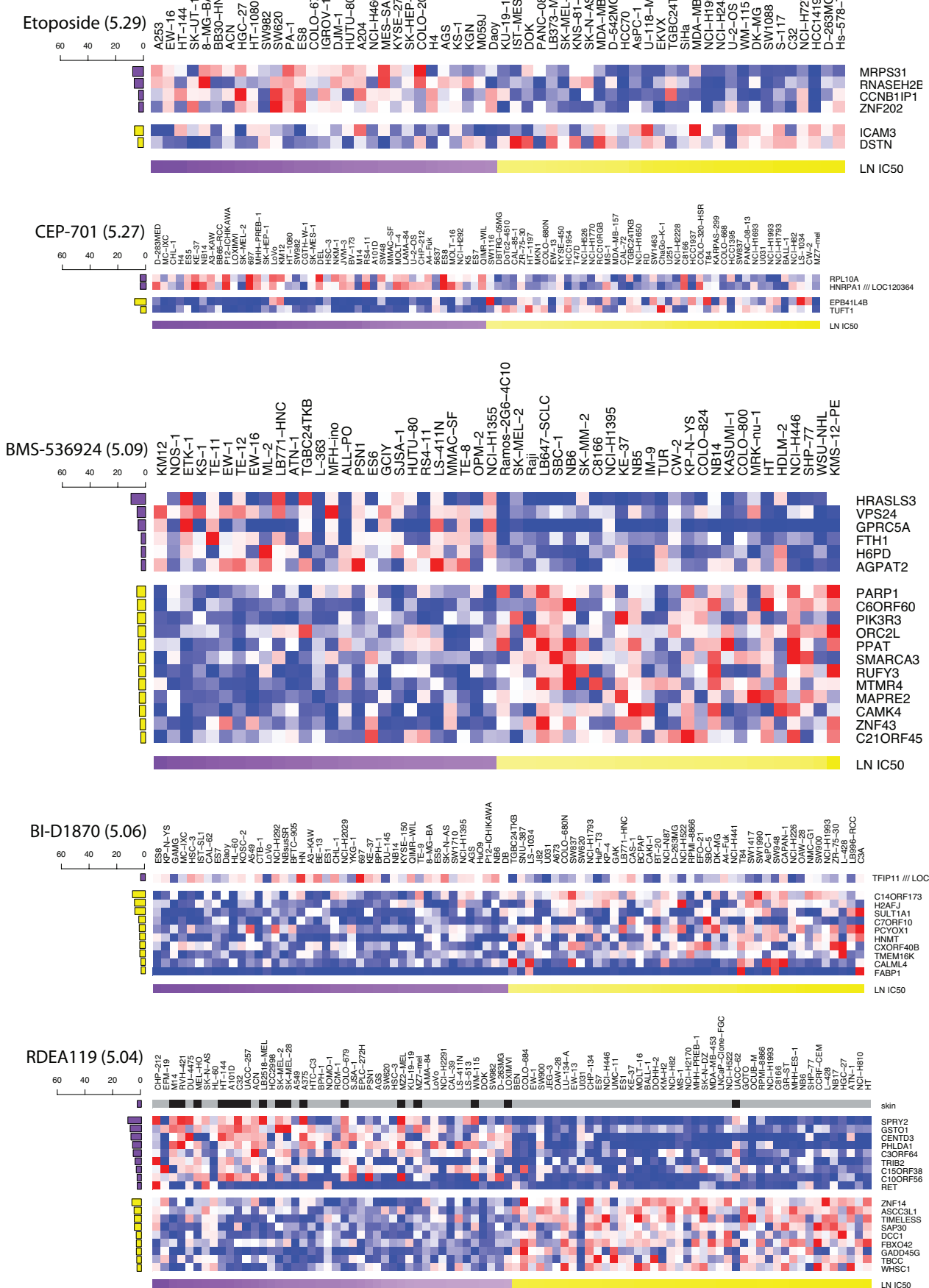


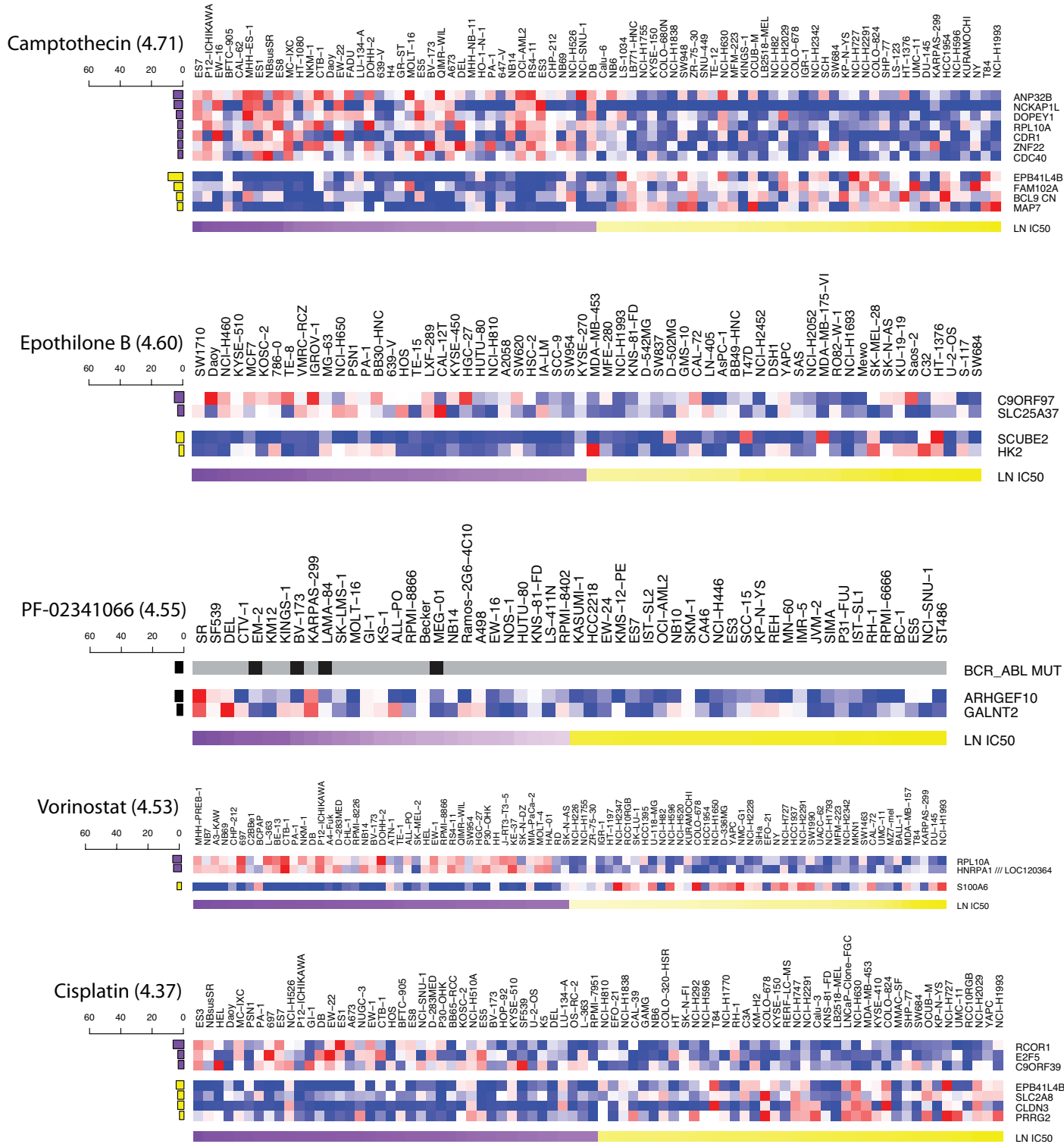




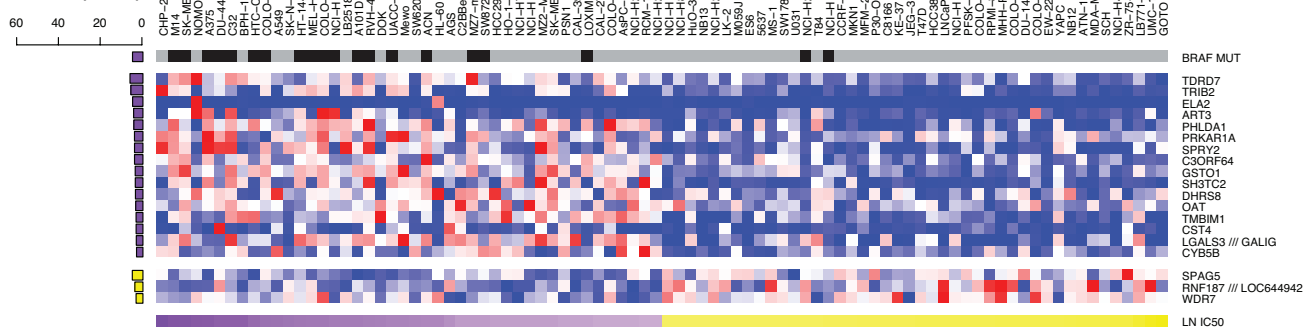




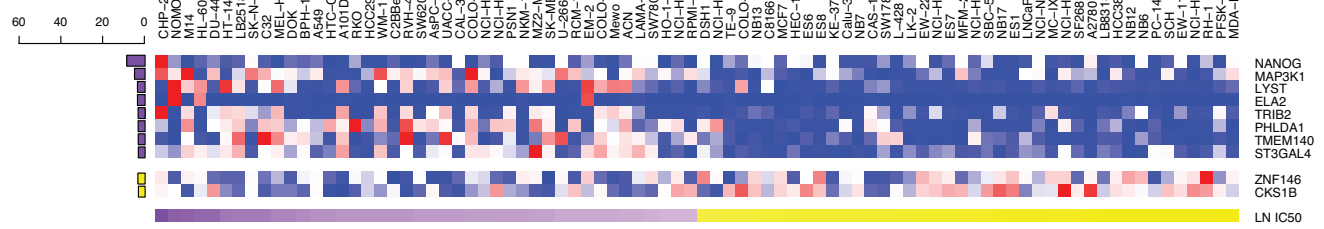




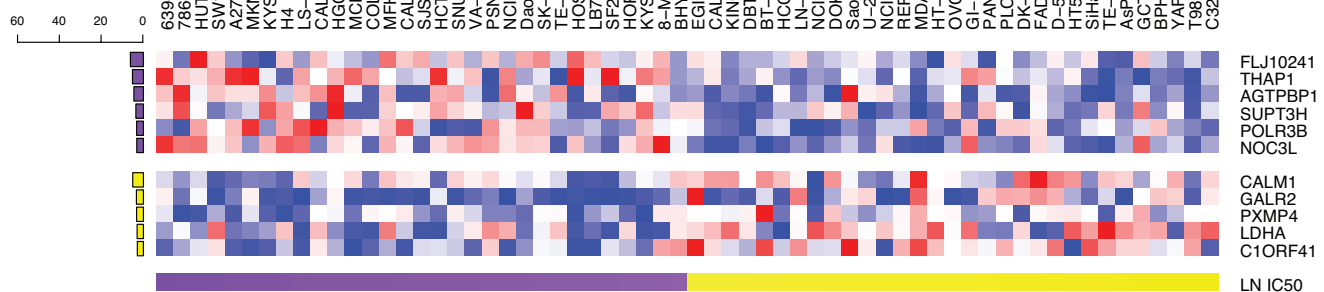
PD-0325901 (4.11)



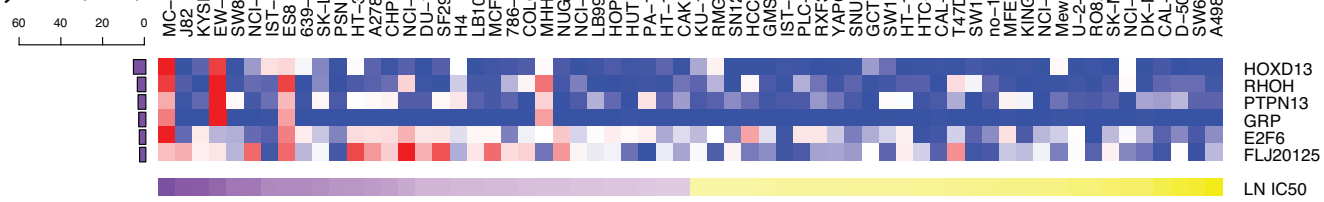
AZD6244 (4.11)



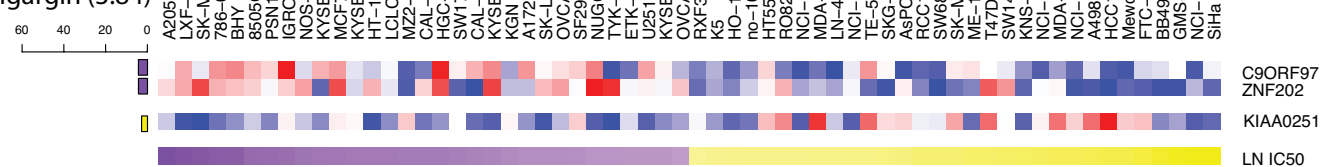
QS11 (3.98)

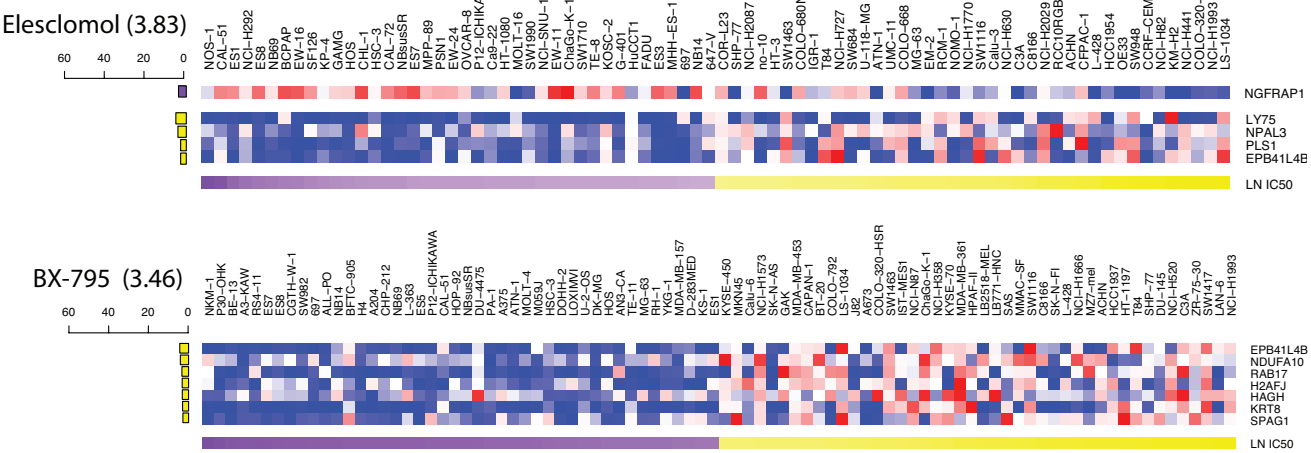


Mitomycin C (3.88)



Thapsigargin (3.84)

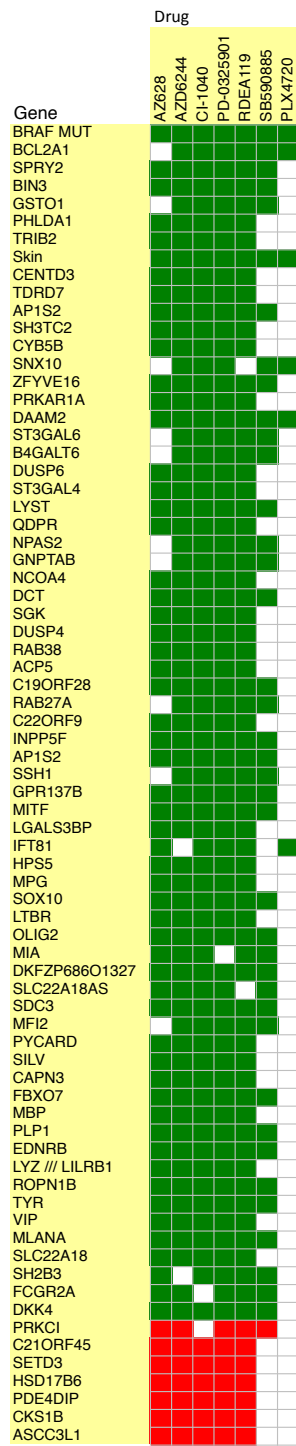




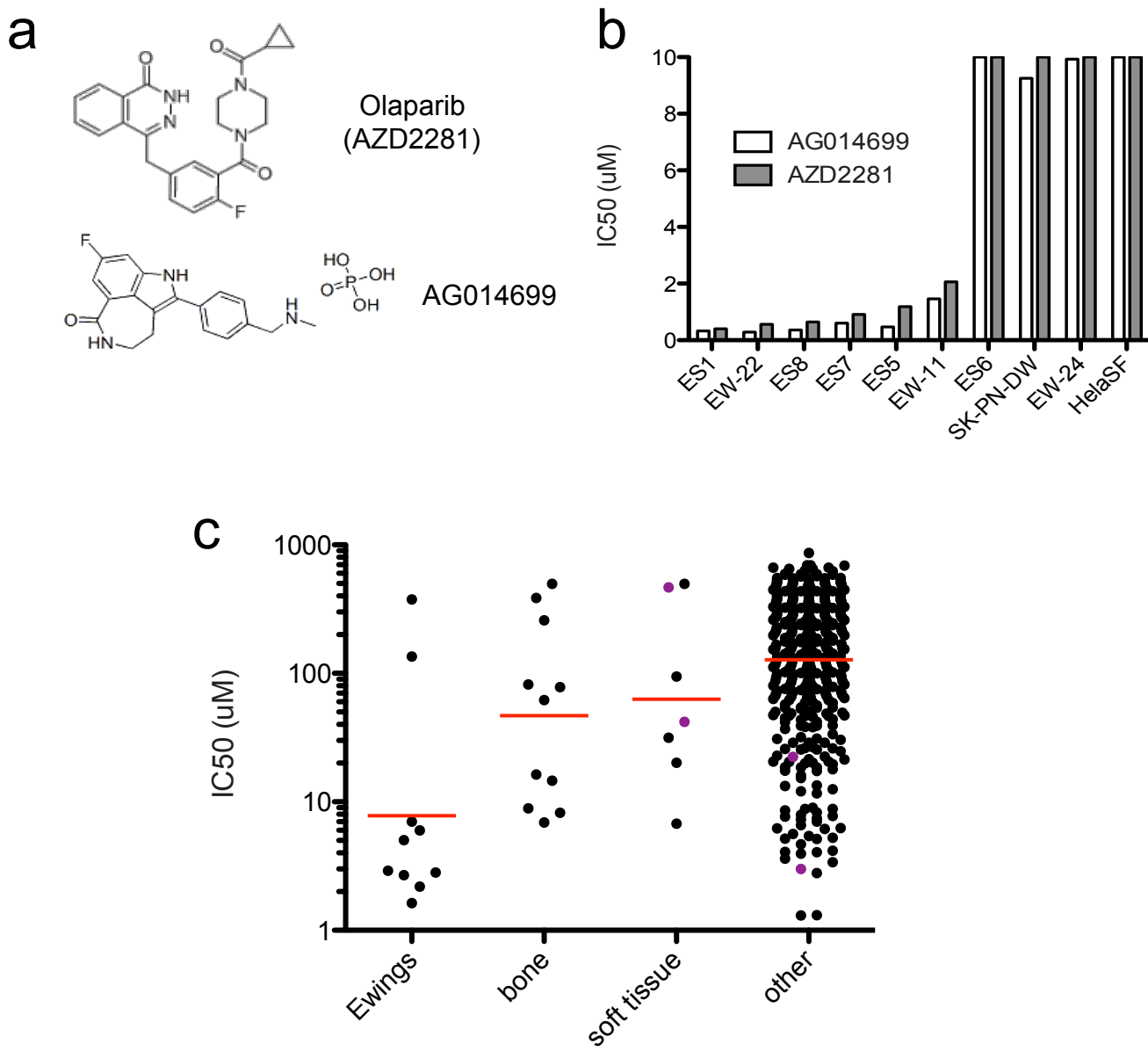
Supplementary Figure 13: Heatmaps for features in marker signatures of all drugs that have at least 2 features with significant effect sizes ($-2.95 > e > 2.79$). Only features with significant effect sizes are shown. Mutation and tissue features are at the top of the heatmap shown in black (sample has feature) and gray (sample lacks feature) followed by sensitivity associated expression and copy number features and finally resistance associated expression and copy number features. To the left of each feature is a barplot indicating the absolute value of the effect size. Bars in purple are negative effects, indicating features associated with sensitivity and bars in yellow are positive effects, indicating features associated with resistance. The natural log IC50 for each cell line is represented at the bottom. Cell lines shown for each heatmap are those with lowest and highest 10% of IC50s for each drug.

Resistance					Sensitivity				
Genes	Drug	Target	Frequency	Effect	Gene	Drug	Target	Frequency	Effect
TP53 MUT	Nutlin-3a	MDM2	1	60.57	BCR_ABL MUT	Dasatinib	ABL, SRC, KIT, PDGFR	1	-61.29
BIN2	Vinorelbine	Microtubules	0.95	53.19		Nilotinib	ABL	1	-52.42
ZNF643	MG-132	Proteasome	1	21.95		WH-4-023	SRC, ABL	0.99	-43.69
RIMBP2	JW-7-52-1	MTOR	1	21.17		Imatinib	ABL, KIT, PDGFR	1	-28.72
	Paclitaxel	Microtubules	1	13.32		GNF-2	BCR-ABL	1	-22.63
	GW843682X	PLK1	0.99	7.34		AZD-0530	SRC, ABL	1	-15.34
ABCB1	Docetaxel	Microtubules	1	20.89		PF-02341066	MET, ALK	0.99	-4.88
	Vinblastine	Microtubules	1	12.91		Axitinib	PDGFR, KIT, VEGFR	1	-3.37
	Vinorelbine	Microtubules	1	11.40	LAG3	GSK-650394	SGK3	1	-29.90
	17-AAG	HSP90	1	4.62	MMP28	Lapatinib	EGFR, ERBB2	1	-27.54
ZNF467	GW843682X	PLK1	0.99	19.48		WZ-1-84	BMX	1	-12.54
	Paclitaxel	Microtubules	1	14.17	ERBB2	Lapatinib	EGFR, ERBB2	1	-26.41
	BI-2536	PLK1/2/3	0.85	8.23		BIBW2992	EGFR, ERBB2	1	-9.34
RB1 MUT	PD-0332991	CDK4/6	1	18.10	PERLD1	Lapatinib	EGFR, ERBB2	1	-23.70
EPB41L4B	PD-0332991	CDK4/6	1	17.34	BRAF MUT	PLX4720	BRAF	1	-23.25
	Temsirolimus	MTOR	1	10.00		SB690885	BRAF	1	-7.89
	Camptothecin	TOP1	1	9.48		PD-0325901	MEK1/2	1	-4.99
	CEP-701	FLT3, JAK2, NTRK1, RET	1	8.43	NQO1	17-AAG	HSP90	1	-22.21
	NVP-BEZ235	PI3K /mTor	0.97	8.35	ADK	AICAR	AMPK agonist	1	-21.52
	Cisplatin	DNA crosslinker	1	5.00	CDKN2a(p14) MUT	Dasatinib	ABL, SRC, KIT, PDGFR	1	-20.28
	BX-795	TBK1, PDK1, IKK, AURKB/C	1	4.44		WH-4-023	SRC, ABL	0.99	-11.93
	Elesclomol	HSP70	1	2.85	PCSK5	Erlotinib	EGFR	1	-19.60
C1ORF109	Z-LNNle-CHO	g-secretase	1	16.09	TRIM16	Dasatinib	ABL, SRC, KIT, PDGFR	1	-19.27
CCNT2	Dasatinib	ABL, SRC, KIT, PDGFR	1	15.96		AZD-0530	SRC, ABL	1	-3.52
GARNL1	MG-132	Proteasome	1	14.91					
PLAGL2	17-AAG	HSP90	1	13.14					

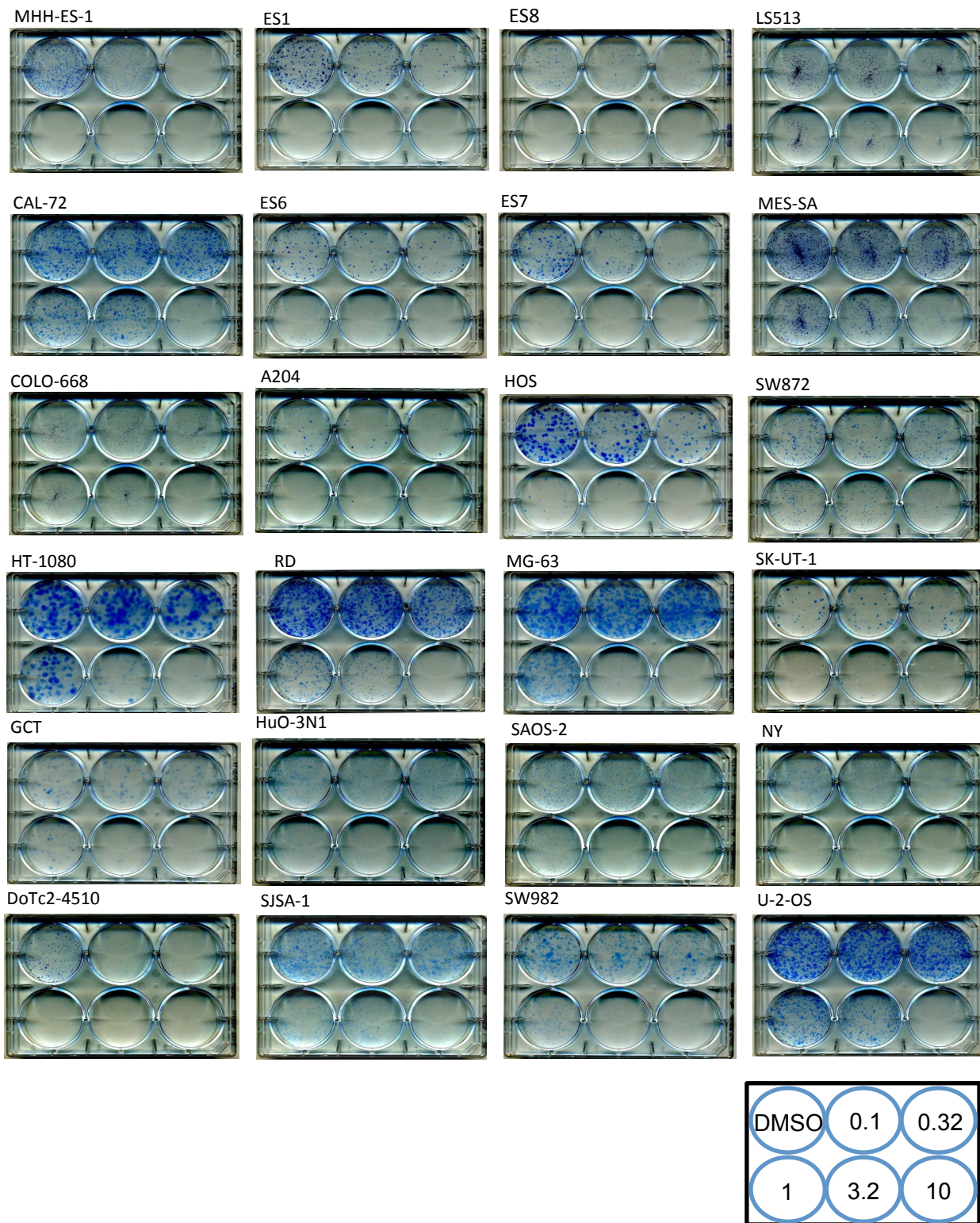
Supplementary Table 3: Highly significant genomic biomarkers of drug response from EN analysis. High frequency features ($f > 0.76$) associated with the largest effect sizes are displayed together with the relevant drug and grouped into positive effect sizes associated with resistance (left) and negative effect sizes associated with sensitivity (right). The top 15 resistance and sensitivity associations are in bold and additional drugs that are associated with each gene at the significance criteria are included in the table.



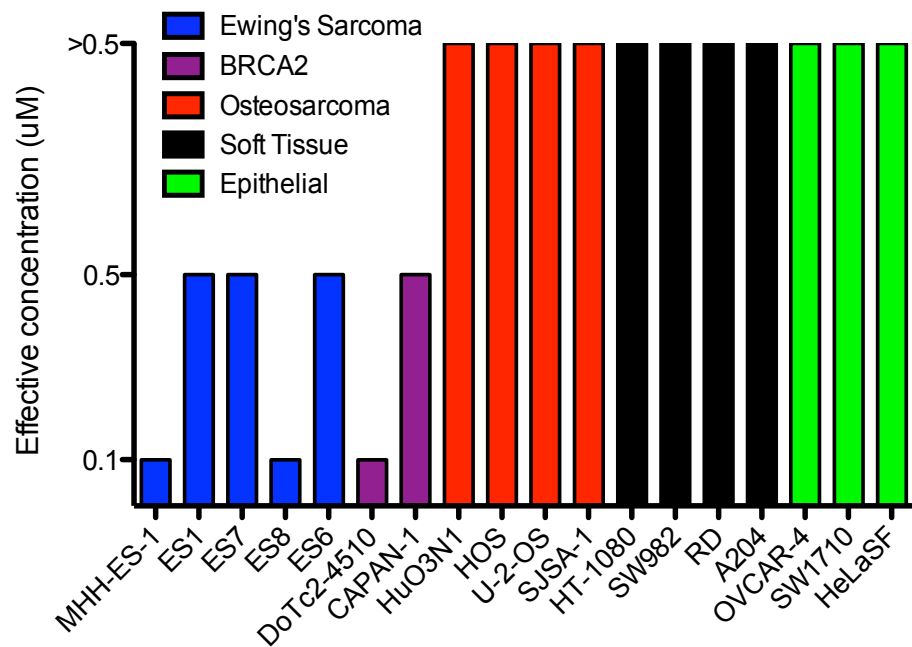
Supplementary Figure 14: Heatmap of recurrent features in RAF and MEK1/2 inhibitor signatures from EN analysis. Green indicates that the feature is associated with drug sensitivity and red indicates association with resistance. Features displayed were present in 5 or more of the 7 RAF and MEK1/2 inhibitors screened.



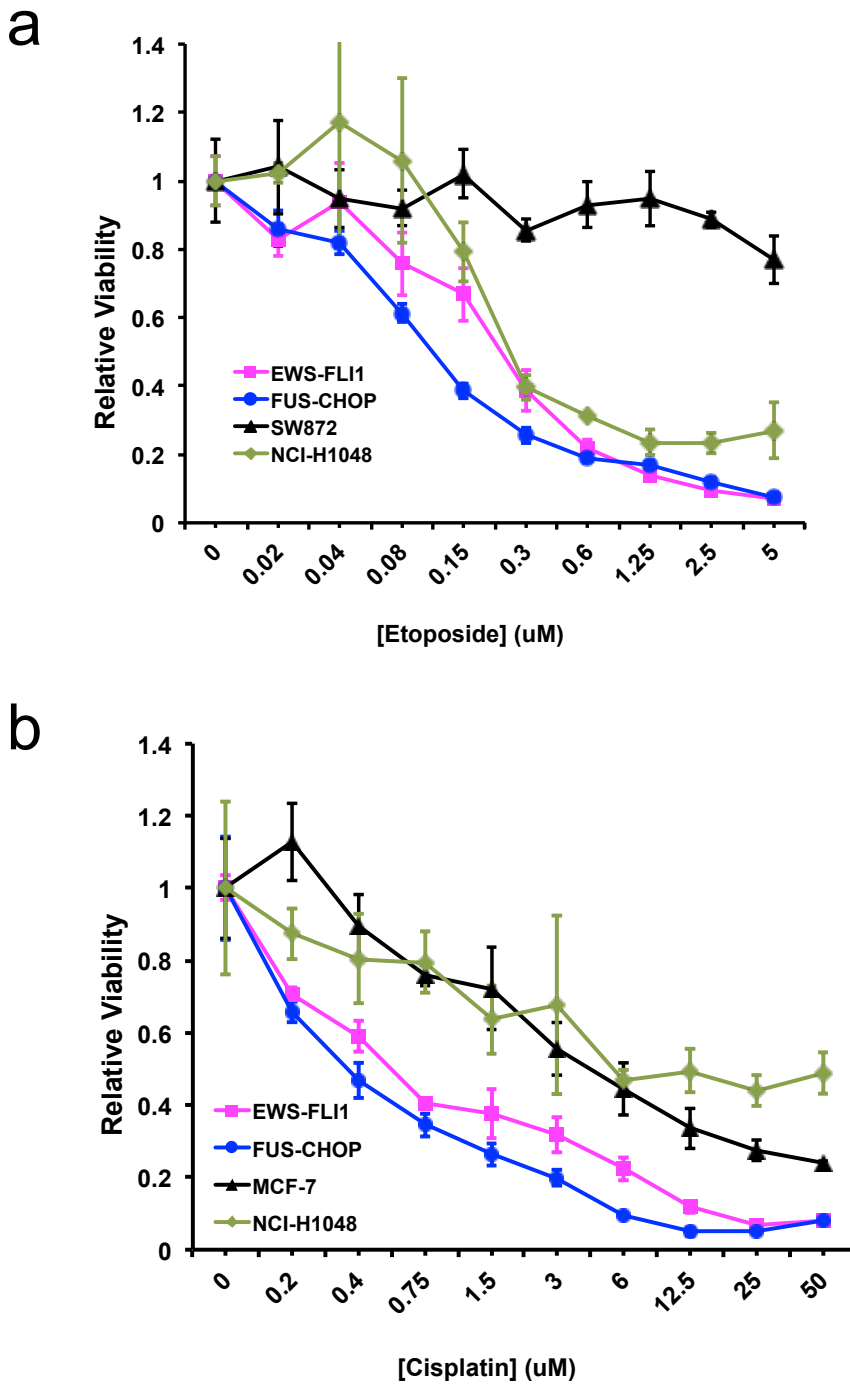
Supplementary Figure 15: Ewing's sarcoma cells are sensitive to multiple PARP inhibitors. **a**, Chemical structures of PARP inhibitors olaparib and AG014699 used in this study. **b**, Comparison of IC₅₀ values of Ewing's cells to olaparib and AG014699 in a 6-day viability assay. IC₅₀ values are capped at 10 uM and HeLaSF cells are included as a negative control. The majority of Ewing's sarcoma cells are acutely sensitive to PARP inhibitors but some cells do not respond in this assay. **c**, Ewing's sarcoma cells show marked sensitivity to olaparib compared to other bone and soft tissue cancers. A scatter plot of cell line IC₅₀ values ($n = 459$) to olaparib on a log scale is shown and the red line indicates the geometric mean. Purple circles are cell lines which have the *EWS-FLI1* rearrangement but historically have not been classified histologically as Ewing's.



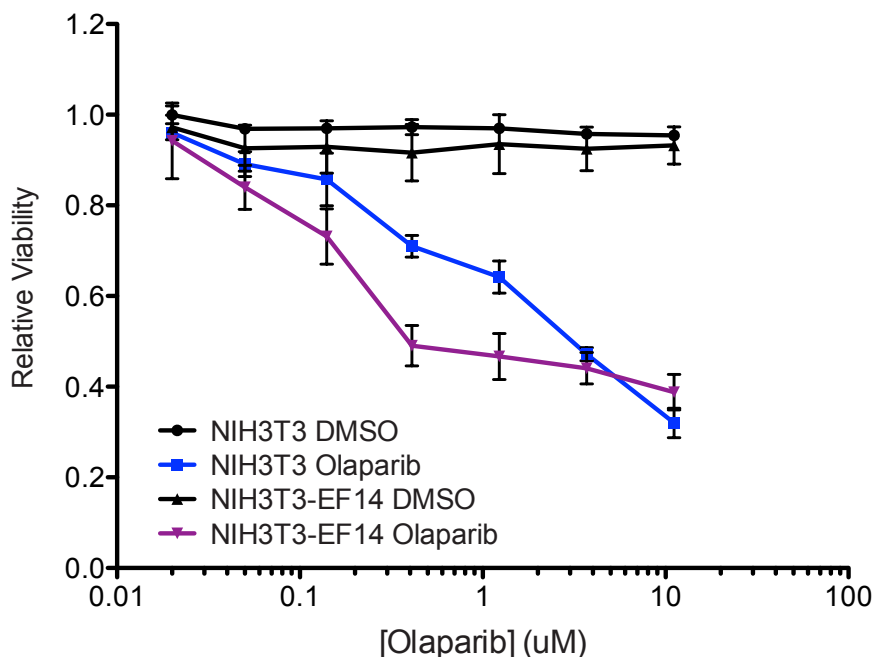
Supplementary Figure 16: Images of olaparib clonogenic assays for Ewing's sarcoma and control cell lines. Clonogenic assays were performed in the presence of increasing concentrations of olaparib (0.1, 0.32, 1, 3.2 or 10 μ M final concentration). Plates were re-drugged every 4 days and fixed and stained 7-21 days following plating. The name of each cell line is given and a schematic (lower right) shows the concentration used for each well.



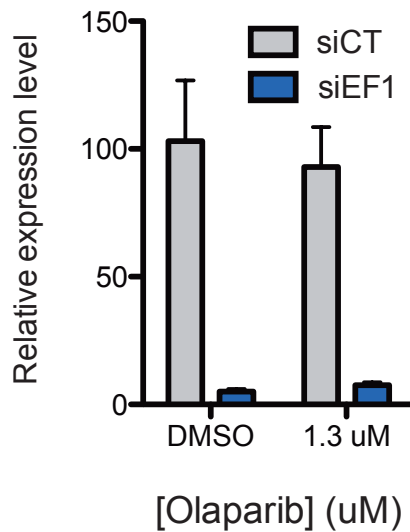
Supplementary Figure 17: Ewing's sarcoma cells are sensitive to PARP inhibitor AG014699 in colony formation assays. Cell lines were treated with 0.1 uM or 0.5 uM AG014699 for 7-21 days with re-druging every 3-4 days. For each cell line the concentration necessary to reduce colonies >90% relative to controls is plotted.



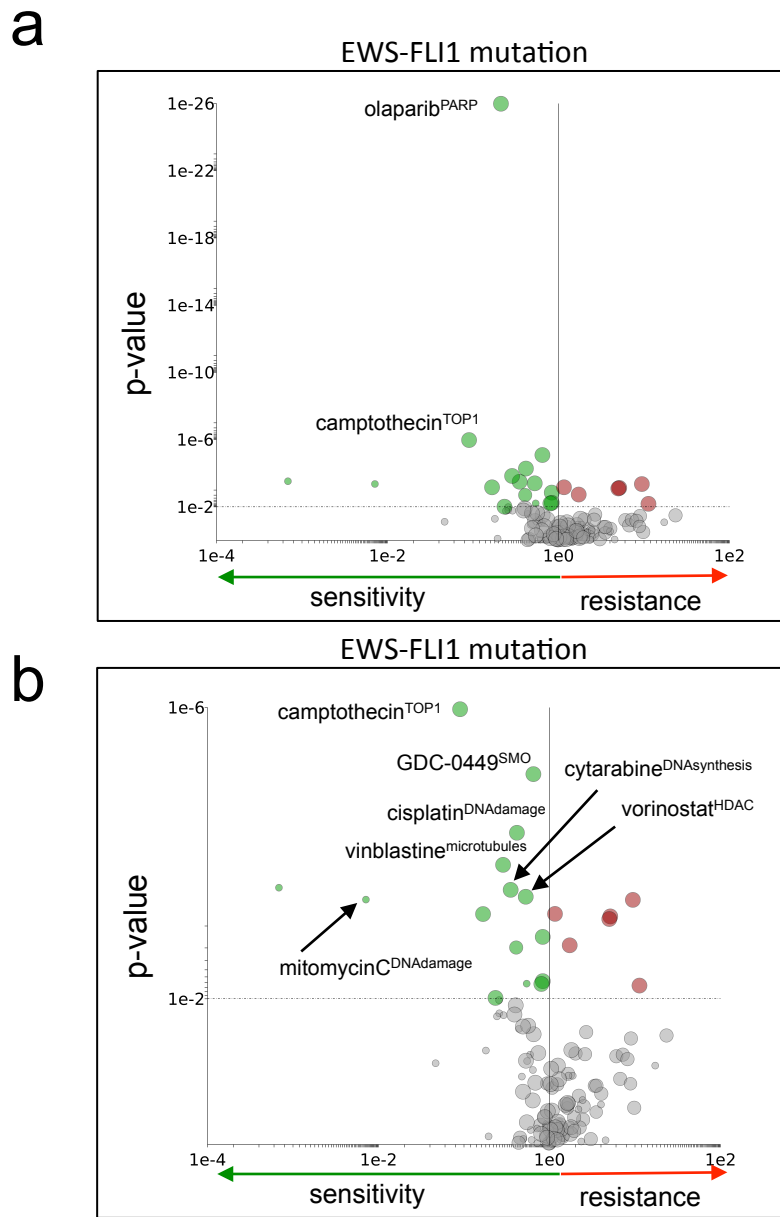
Supplementary Figure 18: *EWS-FLI1* transformed mouse mesenchymal cells are not sensitised to etoposide or cisplatin. As a control we show dose response curves to **a**, etoposide or **b**, cisplatin comparing the sensitivity of *EWS-FLI1* and *FUS-CHOP* transformed mouse mesenchymal cells. Human non-mesenchymal cell lines were included as an additional control. Each drug concentration was assayed in triplicate and error bars represent s.d.



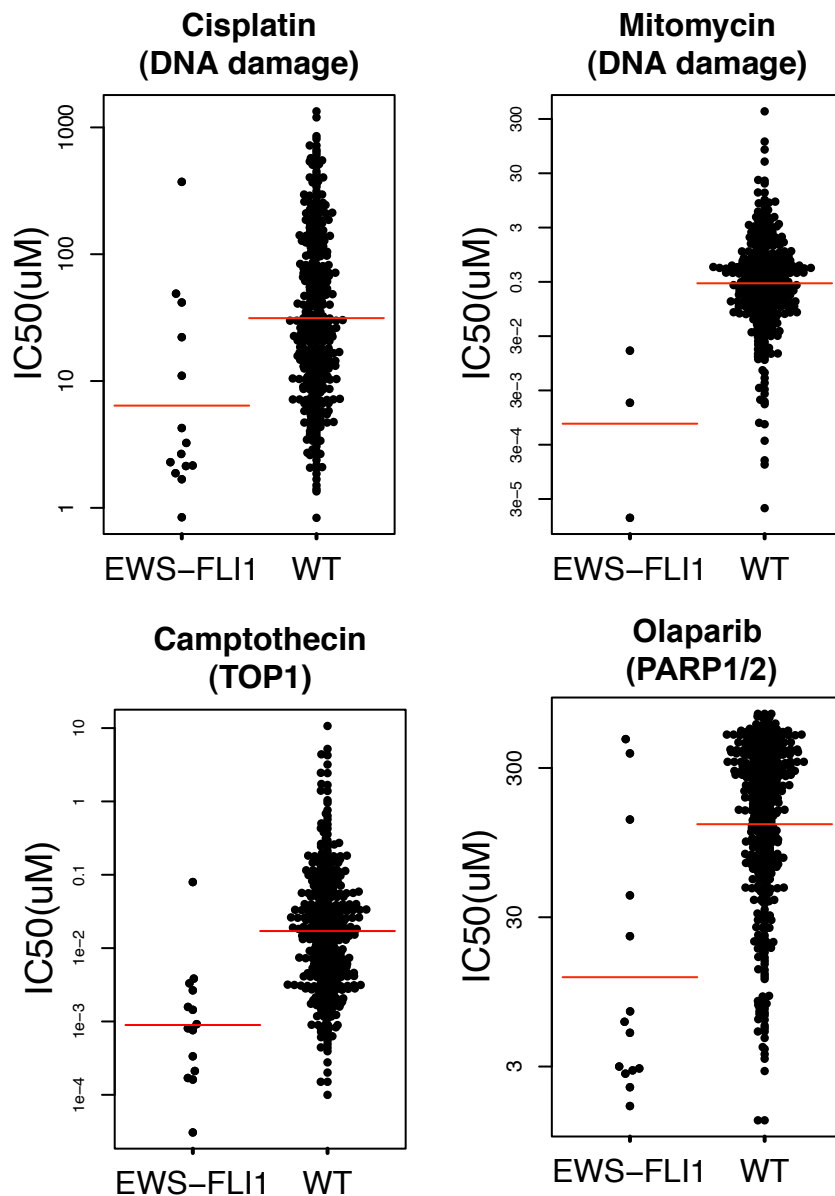
Supplementary Figure 19: EWS-FLI1 expression is specifically associated with PARP inhibitor sensitivity. Olaparib dose response curves of NIH3T3 cells stably expressing EWS-FLI1 (NIH3T3-EF14) or the parental control line. Expression of EWS-FLI1 increased sensitivity to olaparib. The effect was greatest at low doses of olaparib whereas at higher doses both cell lines were sensitive presumably due to general cellular toxicity. Viability was normalised to untreated cells. Each drug concentration was assayed in triplicate and error bars represent the s.d.



Supplementary Figure 20: Confirmation of siRNA-mediated depletion of EWS-FLI1 in A673 cells. A673 were transfected with either control (siCT) or EWS-FLI1 (siEF1) siRNA for 72 hours and cells were concomitantly treated with either olaparib or DMSO. Relative expression levels of EWS-FLI1 (normalized to ribosomal protein RPLP0) were assessed by RT-QPCR. Expression was assayed in triplicate and errors bars are s.d.



Supplementary Figure 21: The *EWS-FLI1* rearrangement is associated with sensitivity to cytotoxic drugs. **a** and **b**, *EWS-FLI1* mutation-specific volcano plots of drug sensitivity from MANOVA. The drug name is indicated and therapeutic drug target(s) (in superscript) are indicated for selected data. Circle size is proportional to the number of mutant cell lines screened (max = 14 for **a** and **b**). For **b** the data for olaparib has been removed to make less significant associations clear (note the change to scaling on y-axis).



Supplementary Figure 22: Association of the *EWS-FLI1* translocation with sensitivity to DNA damaging agents. Scatter plots of IC_{50} values from selected associations from the MANOVA of *EWS-FLI1* with cytotoxic drugs. The data for olaparib (AZD-2281) is also included for comparison. The cell line IC_{50} values (μM) for each drug are given comparing mutated (MUT) or non-mutated (WT) cell lines. Each circle represents the IC_{50} of one cell line plotted on a log scale and the red bar is the geometric mean. The drug name is indicated above each plot and target(s) are given in brackets.